

## Electronic Supplementary Information

### Orbital and Free Energy Landscape Expedition towards the Unexplored Catalytic Realm of Aromatically Modified FLPs for CO<sub>2</sub> Sequestration

*Mohmmad Faizan, Madhumita Chakraborty, Dinesh Bana, and Ravinder Pawar\**

Laboratory of Advanced Computation and Theory for Materials and Chemistry,

Department of Chemistry, National Institute of Technology Warangal (NITW), Warangal,  
Telangana-506004, India.

[ravinder\\_pawar@nitw.ac.in](mailto:ravinder_pawar@nitw.ac.in)

### Table of Contents

<b>Section S1. Detailed electronic structure analysis of the proposed IFLPs</b>	2
<b>Section S2. Detailed analysis of the CMs obtained in the reaction of CO<sub>2</sub> with proposed IFLPs</b>	5
<b>Section S3. IRC Pathways for the reaction of CO<sub>2</sub> with considered IFLPs.</b>	6
<b>Section S4. Optimized geometries of the CO<sub>2</sub> adducts formed in the reactions.</b>	9
<b>Section S5. Detailed analysis of NICS(0) and AICD of 5 and 6</b>	9
<b>Section S6. Orbital change plots along the IRC.</b>	12
<b>Section S7. Detailed PIO analysis of 5 and 6</b>	13
<b>Section S8. Variation in important distances throughout the metadynamics simulation</b>	16
<b>Section S9. 3-D FES and relative free energy profile along the MEP obtained from the metadynamics simulations</b>	19
<b>Section S10. FES analysis for the cases of 5 and 6</b>	21
<b>Section S11. Optimized cartesian coordinates of the structures obtained in the reaction of CO<sub>2</sub> with the proposed IFLPs.</b>	26

## Section S1. Detailed electronic structure analysis of the proposed IFLPs

The optimized geometries of the investigated IFLPs with appropriate labels and important geometrical parameters are depicted in Figure S1. The important natural bond orbitals (NBOs) and the AICD plots with NICS(0) values of the respective IFLPs are also given in Figure S1. The cartesian coordinates of the optimized structures have also been provided in the Section S11.

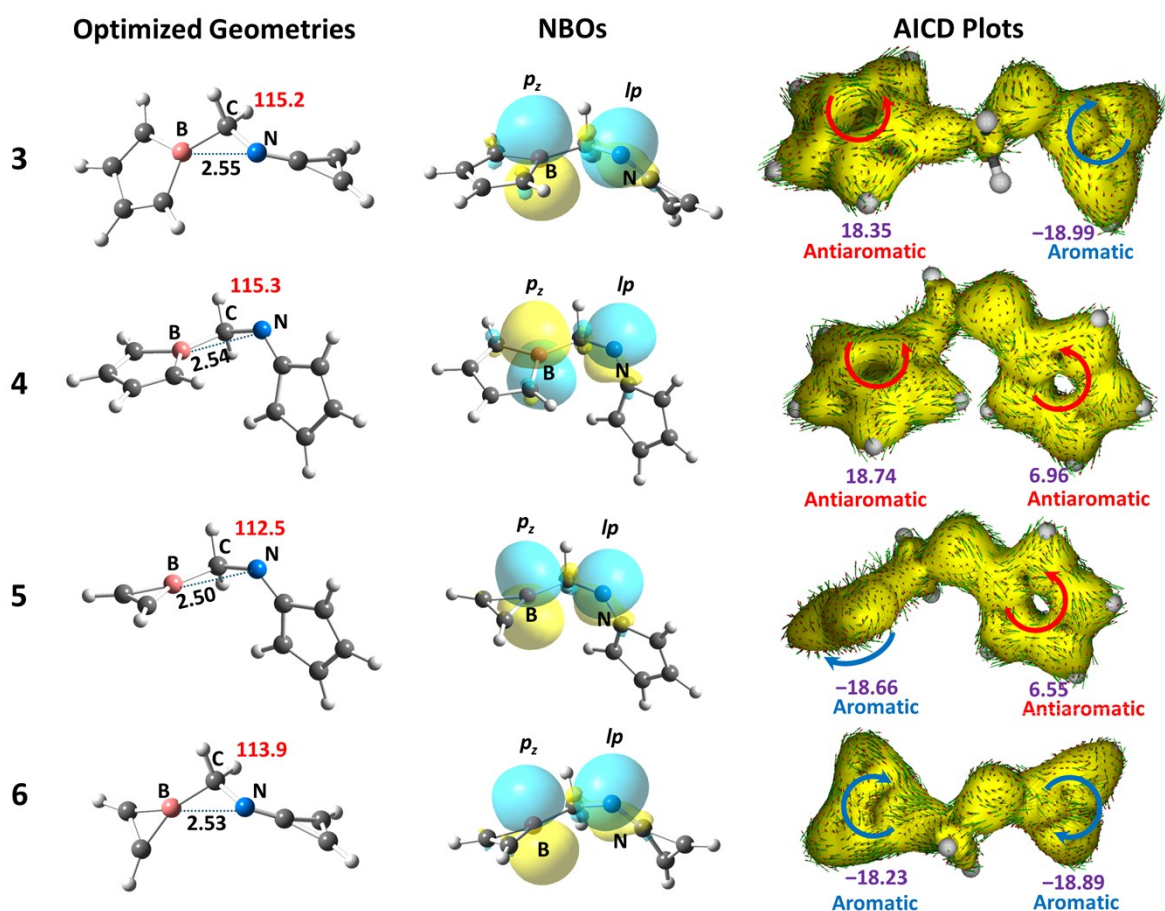


**Figure S1.** Optimized geometries, Natural bond orbitals (NBOs) and AICD plots of the considered IFLPs. (Important geometrical parameters are mentioned with the optimized geometries, numbers in black and red colour are the distances in angstrom and  $\angle$ BCN angles in degrees, the counterclockwise red arrows over the AICD plots represent the paratropic current while the clockwise blue arrows represent the diatropic current and the NICS(0) (ppm) values of the respective rings are given as numbers in purple colour below the AICD plots, NBOs and AICD surfaces are plotted at 0.01 and 0.4 a. u. iso values)

It can be observed from the optimized geometries of the proposed IFLPs given in Figure S1 that the BN distances and  $\angle$ BCN angles are  $\sim 2.55$  Å and  $\sim 115^\circ$ , respectively in each case, which are greater than in case of **1** reported earlier. It can also be intuitively observed from the optimized structures that the coordinating sites of the B and N atoms are not directing towards each other. The same fact can also be inferred from the orientation of the  $p_z$  and  $lp$  orbitals at B and N atoms of the IFLPs observed in the NBO plots in Figure S1. The  $p_z(\text{B})$  and  $lp(\text{N})$  orbitals were found to be oriented nearly parallel to each other. Unlike **1**, no orbital charge transfer (OCT) from  $lp(\text{N})$  to  $p_z(\text{B})$  orbital has been found in any of the proposed IFLPs. The lack of OCT between  $lp(\text{N})$  and  $p_z(\text{B})$  indicates the absence of prior frustrated state in the investigated IFLPs as observed in the case of **1**. The prior state of frustration is highly subjective to the steric environment of the acidic and basic sites and can be controlled by appropriate substitution which is out of the scope of the present work. However, the simultaneous existence of  $lp(\text{N})$  and  $p_z(\text{B})$  orbitals at  $\alpha$ -position to each other in parallel orientation warrants the synergic action of the acidic and basic sites which is the inherent characteristic of the FLPs. Thus, the basic site i.e., N atom of the IFLPs interact with the electrophilic C atom of the  $\text{CO}_2$  molecule by the donation of lone pair electrons causing excess negative charge at O atom of the  $\text{CO}_2$  molecule. The excess charge developed at the O atom compensated by the empty  $p_z$  orbital at the acidic site i.e., B atom of the IFLPs. Aromatically tempering the acidity and basicity of the reactive sites may not only affect the reactivity but also lead to severe changes in the catalytic behaviour, which is the primary focus of the present work.

Further, to have initial idea about the aromatic or anti aromatic nature of the borole, borirene, cyclopropenimine and cyclopentadienylimine fragments of the examined IFLPs, NICS(0) at the geometrical centres of the respective rings has been calculated. The anisotropy of the induced current (AICD) has also been plotted to visualize the circulation of the current vectors in the respective rings. The NICS(0) values of the borole fragment in **3** and **4** were found to be 18.35 and 18.74 ppm, respectively (see Figure S1). The positive NICS(0) values and strong paratropic ring current (i.e., anti-clockwise current vectors, Figure S1) of the borole fragments signifies the antiaromatic character at the acidic sites of **3** and **4**. Likewise, comparatively weak paratropic ring current along with NICS(0) values of 6.96 and 6.55 ppm for the cyclopentadienylimine fragment in **4** and **5** has been observed (see Figure S1). The smaller NICS(0) values and weak ring current indicates a lower antiaromatic character in the cyclopentadienylimine fragment of **4** and **5** than the borole fragment of **3** and **4**. For borirene

and cyclopropenimine fragments in **3**, **5** and **6**, the NICS(0) value ranges between -18 to -19 ppm along with a strong diatropic current (i.e., clockwise current vectors) highlighting their aromatic character. To evaluate the effect of aromatic or antiaromatic modifications on the acidity and basicity, the hydride ion affinities of the B atom and proton affinities of N atom of the proposed IFLPs have been calculated. The calculated hydride ion and proton affinities are tabulated in Table S1.

**Table S1. Proton affinities (PA) and Hydride ion affinities (HA) of the investigated IFLPs. (All the values are in kcal/mol)**

	PA	HA
<b>3</b>	-232.8	-83.5
<b>4</b>	-219.7	-93.7
<b>5</b>	-220.4	-69.6
<b>6</b>	-233.9	-57.2

The subsequent proton affinities (PA) in case of **3** and **6** were found to be -232.8 and -233.9 kcal/mol, whereas in case of **4** and **5** the PAs were observed to be -219.7 and -220.4 kcal/mol, respectively (see Table S1). The higher PAs in **3** and **6** indicates the higher basicity due the gain in aromatic character at the cyclopropenimine fragment, while the lower PAs of **4** and **5** point towards the decrement in the basicity of N atom due to the gain in antiaromatic character at the cyclopentadienylimine fragment. In **3** and **4** the respective hydride ion affinities (HA) were -83.5 and -93.5 kcal/mol which are greater than the HAs observed in case of **5** and **6** (see Table S1). The greater HAs of **3** and **4** signifies greater acidity due the loss in antiaromatic character at the borole fragment, whereas the lower HA of the **5** and **6** shows diminished acidity because of the loss in aromaticity at the borirene fragment. The close inspection of the HAs in Table 1 shows that the HAs in case of **4** and **5** are higher than in **3** and **6**, respectively. This observation shows that the decrement in the basicity of N atom due to the antiaromatic gain at cyclopentadienylimine fragment may significantly enhances the acidity of the B atom. Based on the NICS(0), PA, HA values and AICD the expected changes at the reactive sites during the reaction with CO<sub>2</sub> are displayed in Figure 3 a. In case of **3**, gain in the aromaticity at cyclopropenylimine fragment and the loss in the antiaromaticity at borole fragment has been expected during the reaction with CO<sub>2</sub>. Both changes at the respective fragments are favourable for the stability of the reaction system, thus **3** is expected to be the most reactive among the proposed IFLPs. In contrast, the loss in aromaticity at the borirene fragment and the gain in the antiaromaticity at the cyclopentadienylimine fragment of **5** has

been expected. Both the changes at the rings are unfavourable for the reaction. Hence, **5** is supposed to be the least reactive IFLP, while the reactivity of **4** and **6** is expected to lie in between **3** and **5** as the aromatic gain/loss or antiaromatic gain/loss is favourable for one of the ring fragments.

## Section S2. Detailed analysis of the CMs obtained in the reaction of CO<sub>2</sub> with proposed IFLPs

The optimized geometries of the reactant complexes (CMs) for the reaction of CO<sub>2</sub> with the proposed IFLPs are shown in Figure 4 along with important geometrical parameters. The NBO plots of the CMs and prominent orbital charge transfer (OCT) stabilization energies have also been depicted in Figure S2.

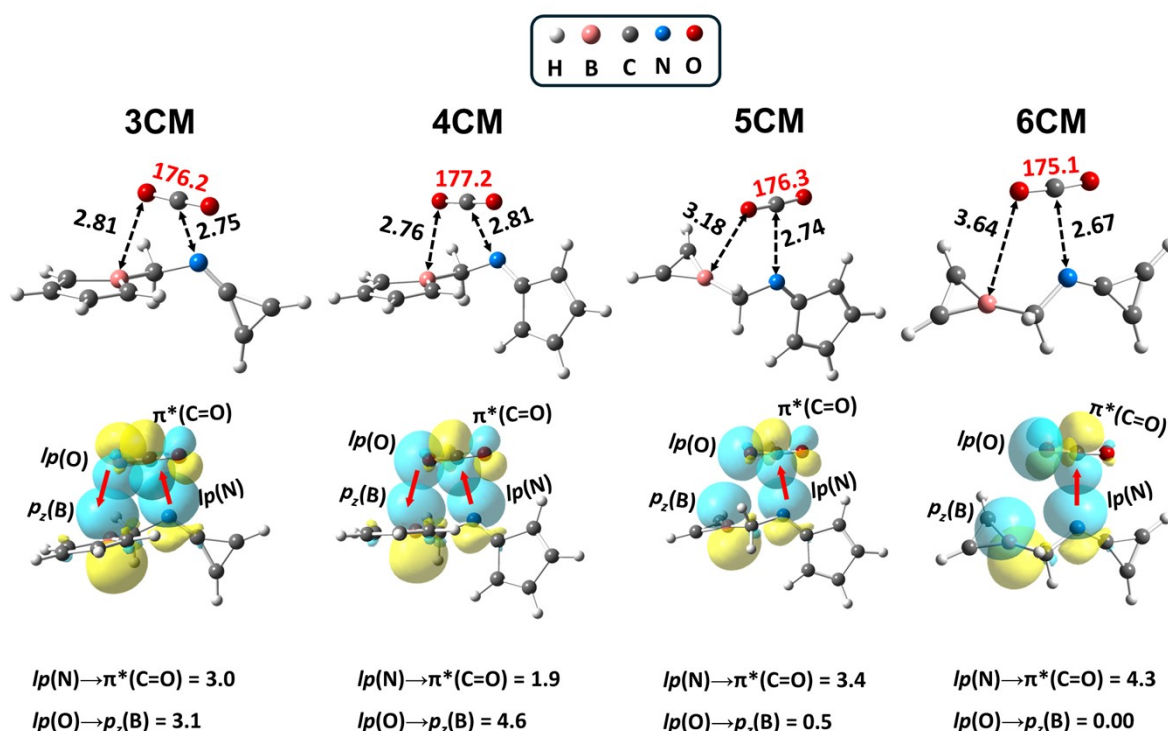


**Figure S2.** Optimized structures and NBO plots of the reactant complexes (CMs) obtained in the reaction of CO<sub>2</sub> with the considered IFLPs. (Numbers in black are the bond distances in Å, numbers in red are the O=C=O bond angle in degrees, the orbital charge transfer given below the NBOs are in kcal/mol, and the red arrows show the direction of charge transfer)

It can be observed in 3CM shown in Figure S2 that the NC distance is 2.75 Å, which is slightly smaller than the BO distance (i.e., 2.81 Å). Although the difference in the NC and BO distances is small but it may provide a minute hint about the initiation of the reaction *via* prior

N-C interaction. In addition to this, similar OCT stabilization energy of  $\sim 3$  kcal/mol from the  $lp(N) \rightarrow \pi^*(C=O)$  and  $lp(O) \rightarrow p_z(B)$  OCTs emphasise nearly equal contribution from the basic and acidic site i.e., N and B atoms of **3**. In comparison to 3CM, the BO distance is found to be  $0.05 \text{ \AA}$  shorter than the NC distance in case of 4CM. Also, the  $lp(O) \rightarrow p_z(B)$  orbital charge transfer with stabilization energy of  $4.6$  kcal/mol has been observed which is greater than the  $lp(N) \rightarrow \pi^*(C=O)$  OCT stabilization energy. These observations indicate the initiation of the reaction from the acidic site of **4**. The contrasting observations in 4CM can be attributed to the decrement in the basicity of the cyclopentadienylimine fragment due to the antiaromatic gain during the interaction with  $CO_2$ . Further, in 5CM and 6CM the NC distances are  $2.74$  and  $2.67 \text{ \AA}$ , which are shorter than the respective BO distances (see Figure S2). The  $lp(N) \rightarrow \pi^*(C=O)$  OCT with stabilization energies of  $3.4$  and  $4.3$  kcal/mol has also been observed in 5CM and 6CM, respectively. No  $lp(O) \rightarrow p_z(B)$  OCT was found in 6CM and observed to be negligible in 5CM (see Figure 4). The shorter NC distance and the absence of  $lp(O) \rightarrow p_z(B)$  OCT clearly shows that the reaction may be initiated dominantly by the prior NC interaction. For **6**, the prior NC interaction in 6CM is obvious because of the increased basicity of the N atom. However, in case of **5**, where the aromatic modulation is unfavourable for the acidic as well a basic site, the prior NC interaction in CM signifies the dominance of the basic site in dictating the reaction pathway.

### Section S3. IRC Pathways for the reaction of $CO_2$ with considered IFLPs.

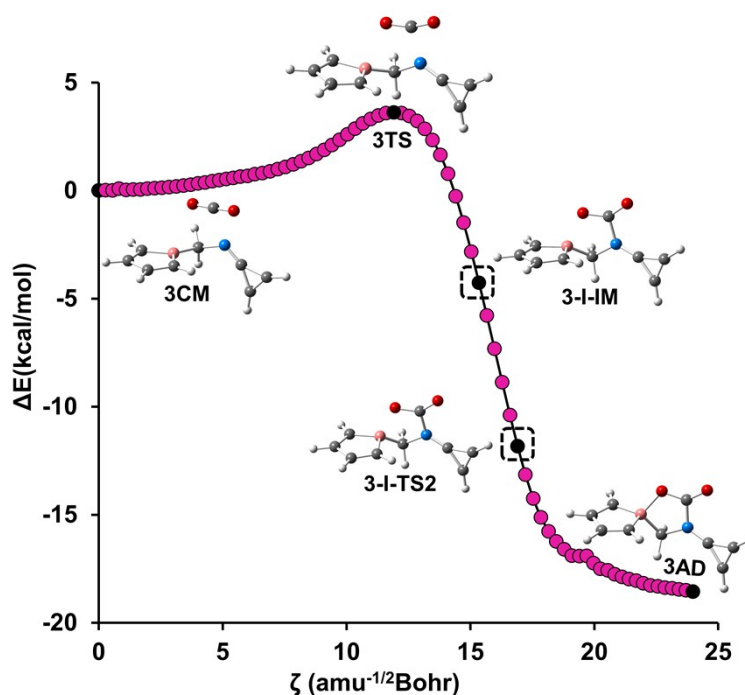


Figure S3. IRC path for the reaction of CO<sub>2</sub> with 3.

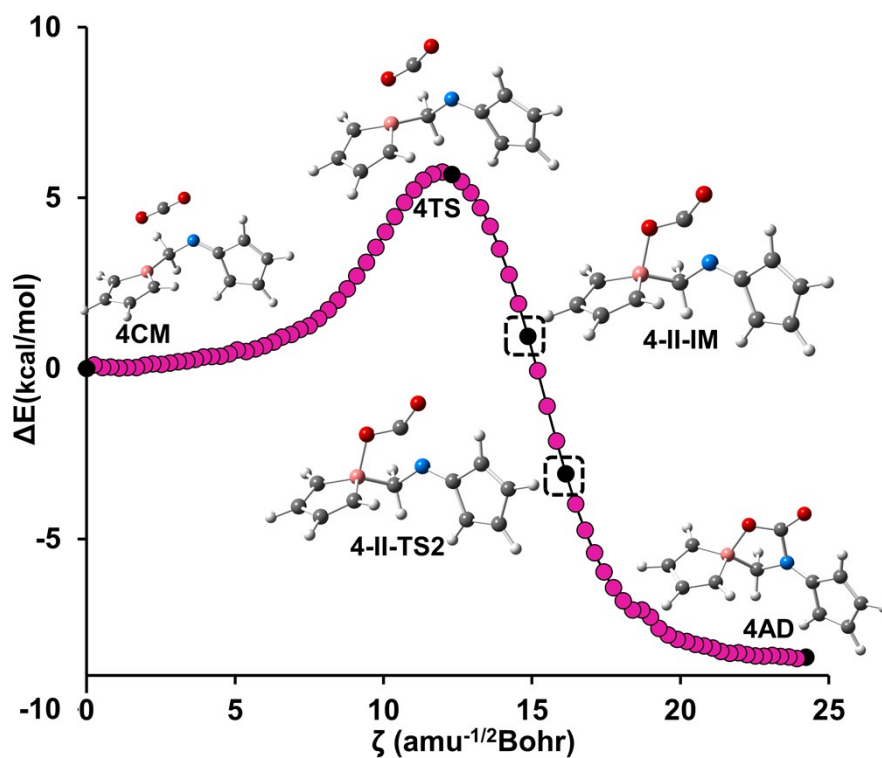


Figure S4. IRC path for the reaction of CO<sub>2</sub> with 4.

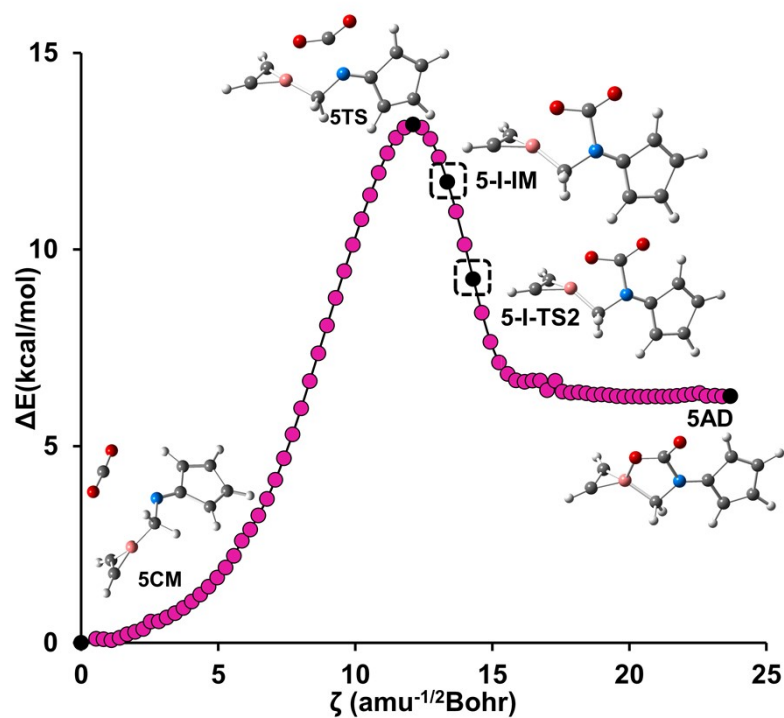


Figure S5. IRC path for the reaction of CO<sub>2</sub> with 5.

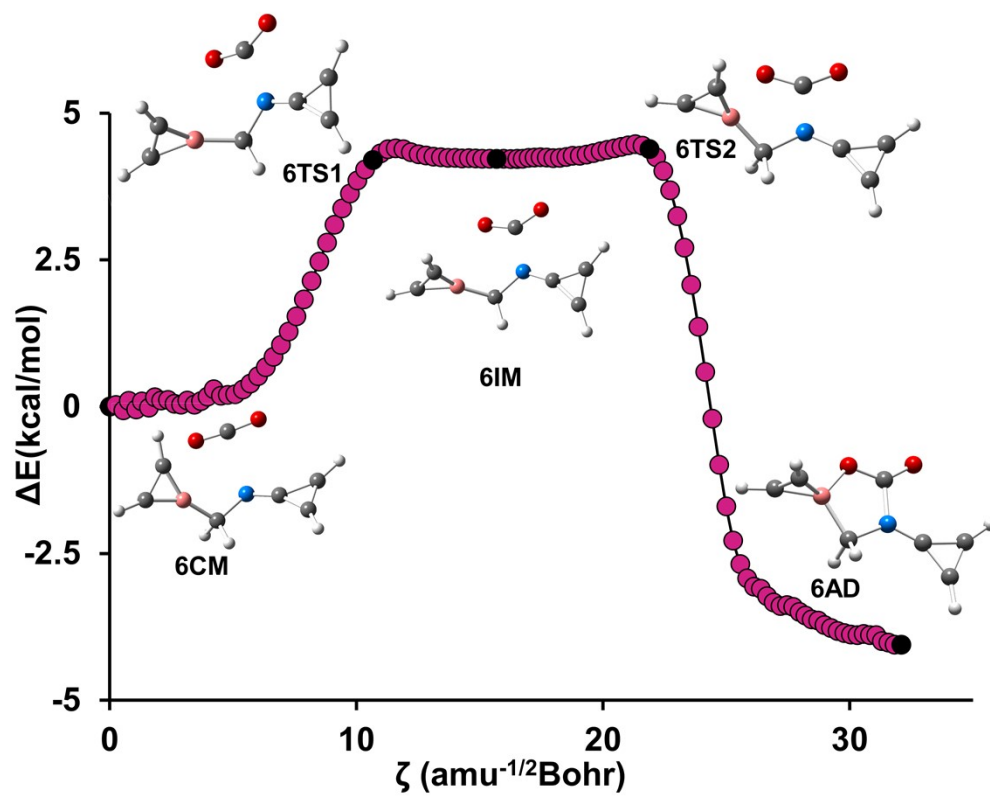
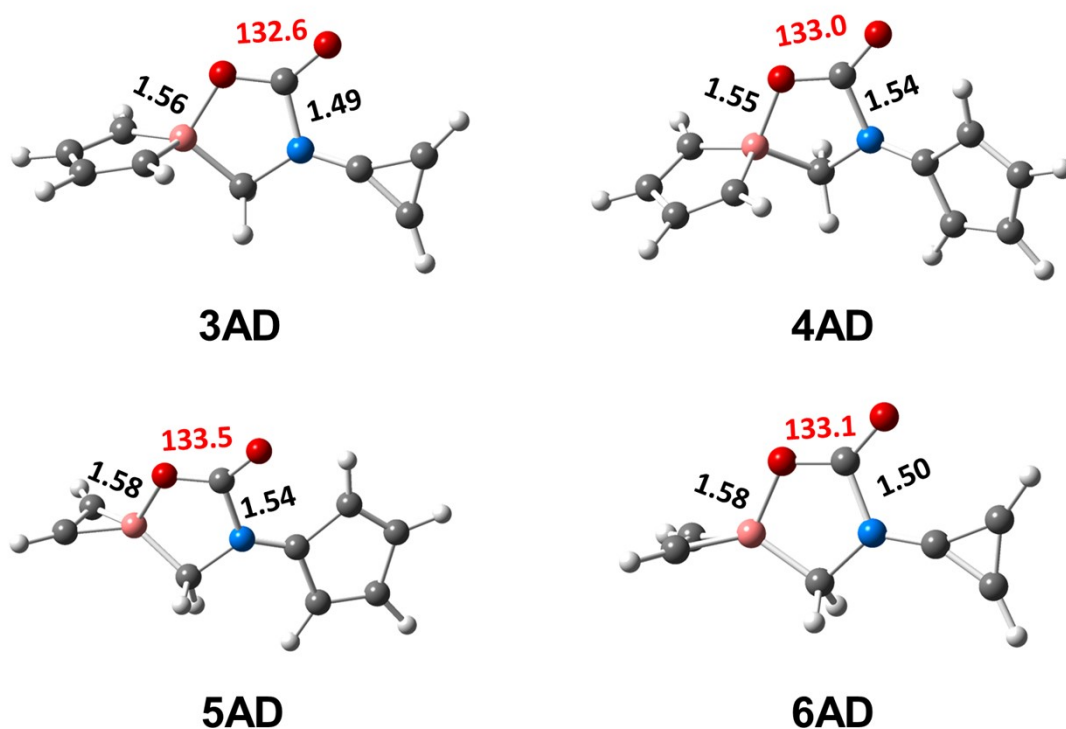


Figure S6. IRC path consisting of the step 1 and 2 for the reaction of  $\text{CO}_2$  with 6.



## Section S4. Optimized geometries of the CO<sub>2</sub> adducts formed in the reactions.



**Figure S7.** Optimized geometries of the adducts obtained in the reaction of CO<sub>2</sub> with proposed IFLPs. (All the numbers in black are the distance in Å and the number in red are the OCO bond angle in degrees)

## Section S5. Detailed analysis of NICS(0) and AICD of 5 and 6

Further, in case of **5**, the increasing antiaromatic character of the cyclopentadienylimine fragment can be inferred by the increasing NICS(0) values and anticlockwise current density vectors along the IRC path shown in Figure S6 and movie S3 given in the ESI. The decreasing aromatic character of the borirene fragment due to the localization of the current vectors over the C=C bond of the borirene ring can also be seen in movie S3. These changes in the ring fragments of **5** are consistent with the electronic structure analysis and supports the increased energy barrier for the activation of CO<sub>2</sub> molecule. Furthermore, the increment in the aromatic character at the cyclopropenimine fragment of **6** can be observed by decreasing NICS(0) values and strengthening of diatropic current (i.e., clockwise current vectors) along the IRC path shown in Figure S7 and movie S4 in the ESI. It can also be noticed from the movie S4 and Figure S7 a that till the formation of 6IM very minute changes occur in the current vectors of the borirene fragment and after the formation the clockwise vectors starts to localize over the

C=C of borirene fragment as observed in case of **5**. This indicates the loss of aromatic character at the borirene fragment and supports the path I followed by the reaction. The variation in NICS(0) of the borirene fragment in **5** and **6** along the IRC has found to be inconsistent with the AICD evolution along the IRC and hence neglected for the qualitative assessment of aromatic loss in the ring.

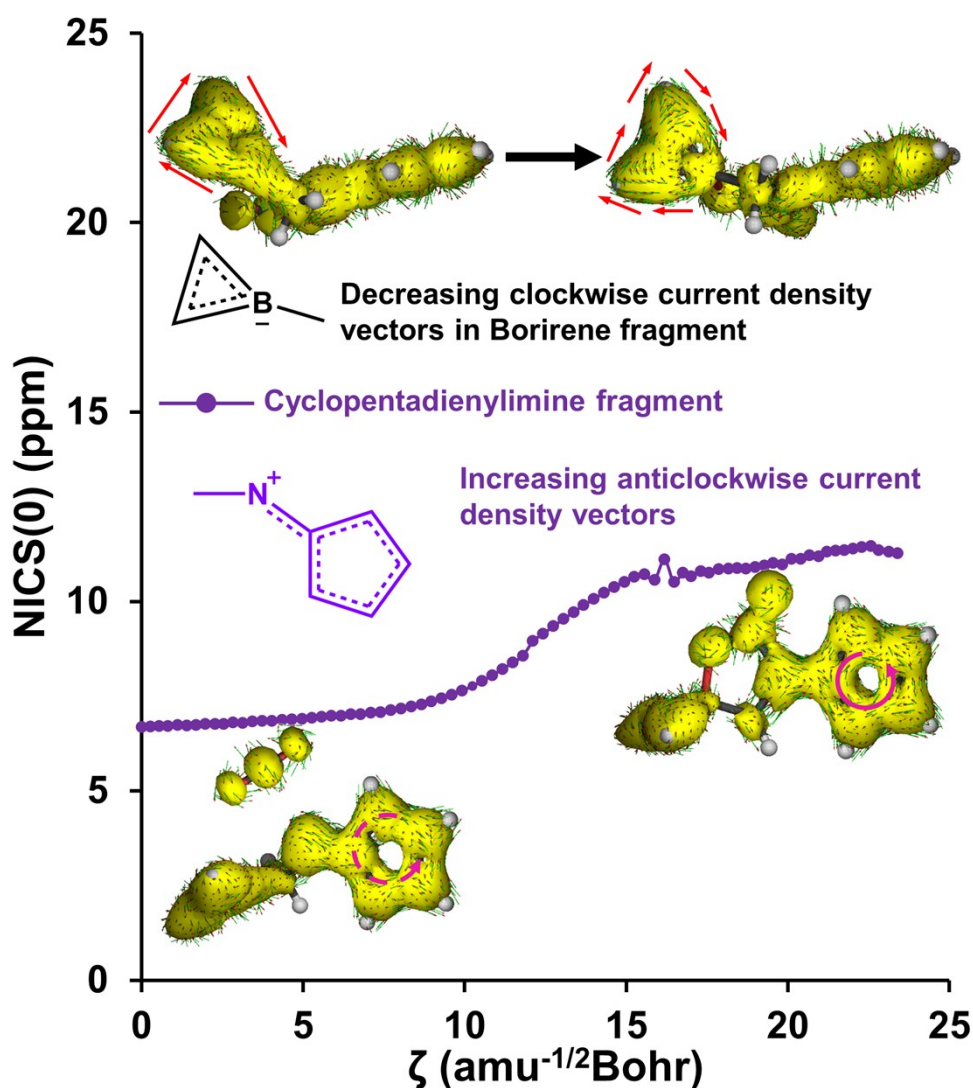


**Figure S8.** Variation in NICS(0) at the geometrical centres of the ring fragments along the IRC paths for the reaction of  $\text{CO}_2$  with **5**. (The AICD plots with the indication of induced current vectors in the respective rings for the initial and final structures obtained in the IRC analysis are also depicted, the direction of arrows over the AICD plots indicates the direction of diatropic or paratropic current, the solid arrow represents the dense current vectors while the dashed arrow represents the dispersed current vectors)

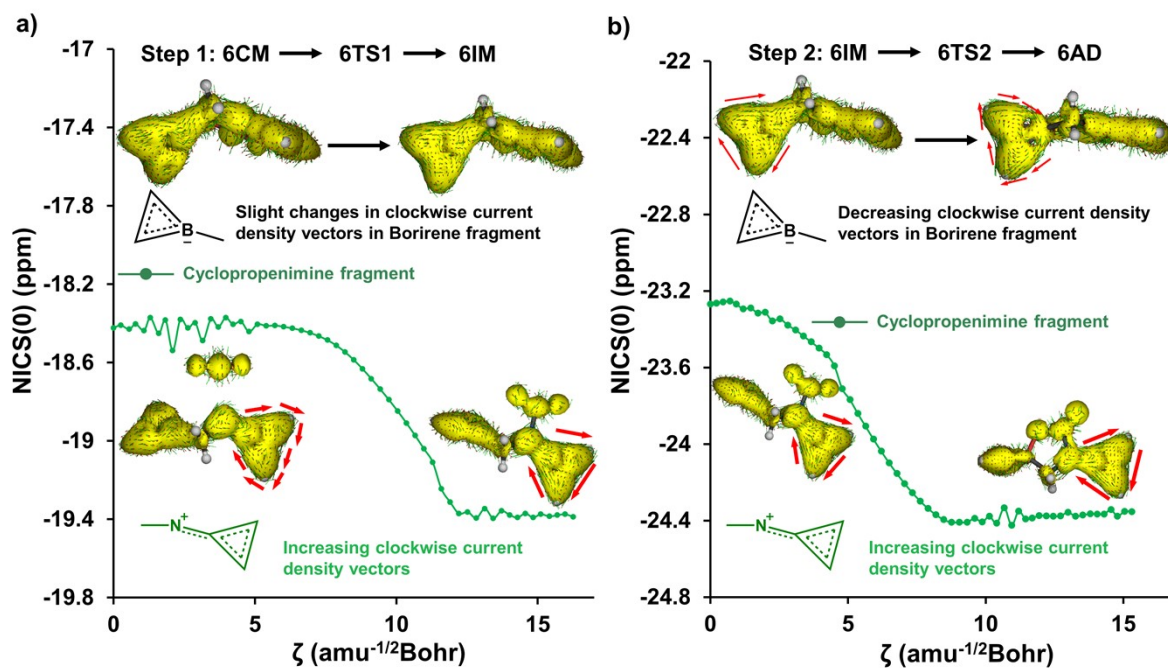


**Figure S9.** Variation in NICS(0) at the geometrical centres of the ring fragments along the IRC paths for the reaction of  $\text{CO}_2$  with **5**. (The AICD plots with the indication of induced current vectors in the respective rings for the initial and final structures obtained in the IRC analysis are also depicted, the direction of arrows over the AICD plots indicates the direction of diatropic or paratropic current, the solid arrow represents the dense current vectors while the dashed arrow represents the dispersed current vectors)

## Section S6. Orbital change plots along the IRC.

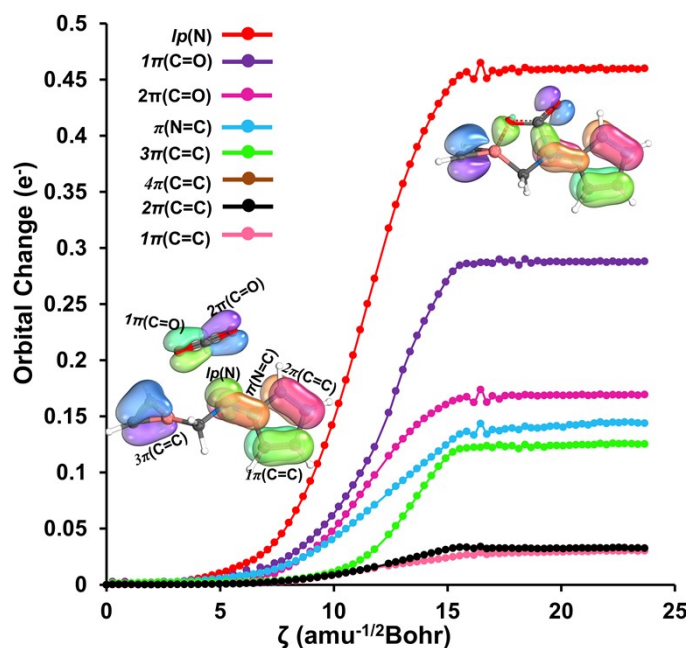


**Figure S10.** The orbital change plots for the reaction of CO<sub>2</sub> with 5 (The IBOs undergoing changes during the reaction are also depicted with appropriate labelling)

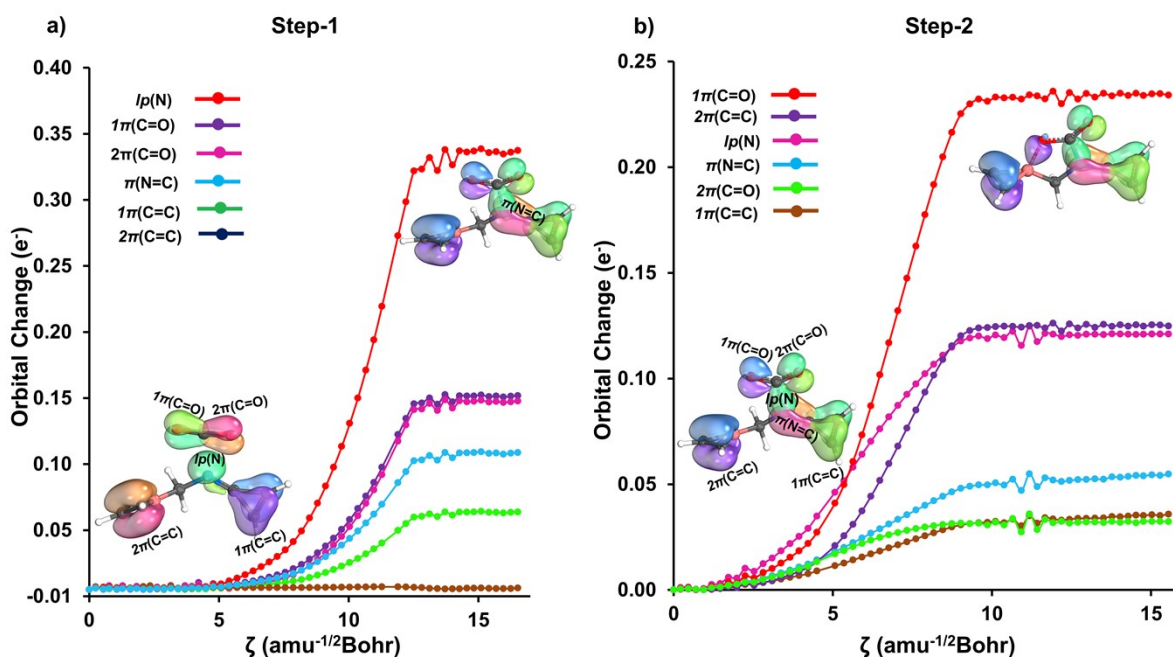


**Figure S11.** The orbital change plots for the reaction of CO<sub>2</sub> with 6 a) step 1 and b) step-2 (The IBOs undergoing changes during the reaction are also depicted with appropriate labelling)

## Section S7. Detailed PIO analysis of **5** and **6**

In case of **5**, the PBI vs IRC plot in Figure S12 imparts the highlights of two important regions (2<sup>nd</sup> and 3<sup>rd</sup>) indicating the important change in the PIO pairs. In 2<sup>nd</sup> region the slope for I PIO pair has found to be greater than II pair, while in 3<sup>rd</sup> the slope for II pair is greater. It is interesting to find that the transition state of the reaction has been observed in the 3<sup>rd</sup> region at  $\zeta = 12.731 \text{ amu}^{-1/2}\text{Bohr}$  of the plot where the variation in PBI of II pair has been increased. These results from the PBI vs IRC plot signifies that the NC interaction brought the reaction close to the transition state after which the BO interaction contributes to the attainment of the transition state. These minute details about the reaction of CO<sub>2</sub> with **5** has also been unrecognised in previous analyses. In the previous analyses (i.e., geometrical, AICD evolution and IBO analysis) the NC interaction has been found to control the activity of **5**. According to PIO along the IRC path, the NC interaction may control the catalytic behaviour, but the control of the catalytic activity has been shifted to the acidic site as soon as the reaction reaches the transition stage. Further, the reaction of CO<sub>2</sub> with **6**, the PBI vs IRC plot shown in Figure S13 comprises two steps. In step 1 of the reaction the NC interaction has been observed to be the prominent interaction as supported by the greater slope values for I PIO pair in 2<sup>nd</sup> region, whereas in step 2 the BO interaction becomes prominent as evident by the slopes in 3<sup>rd</sup> region. The variation in PBI along the IRC path for **6** presents the facts observed in earlier analyses. Thus, the extensive PIO analysis of the reactions along the IRC paths provides hidden details overlooked by other analyses.

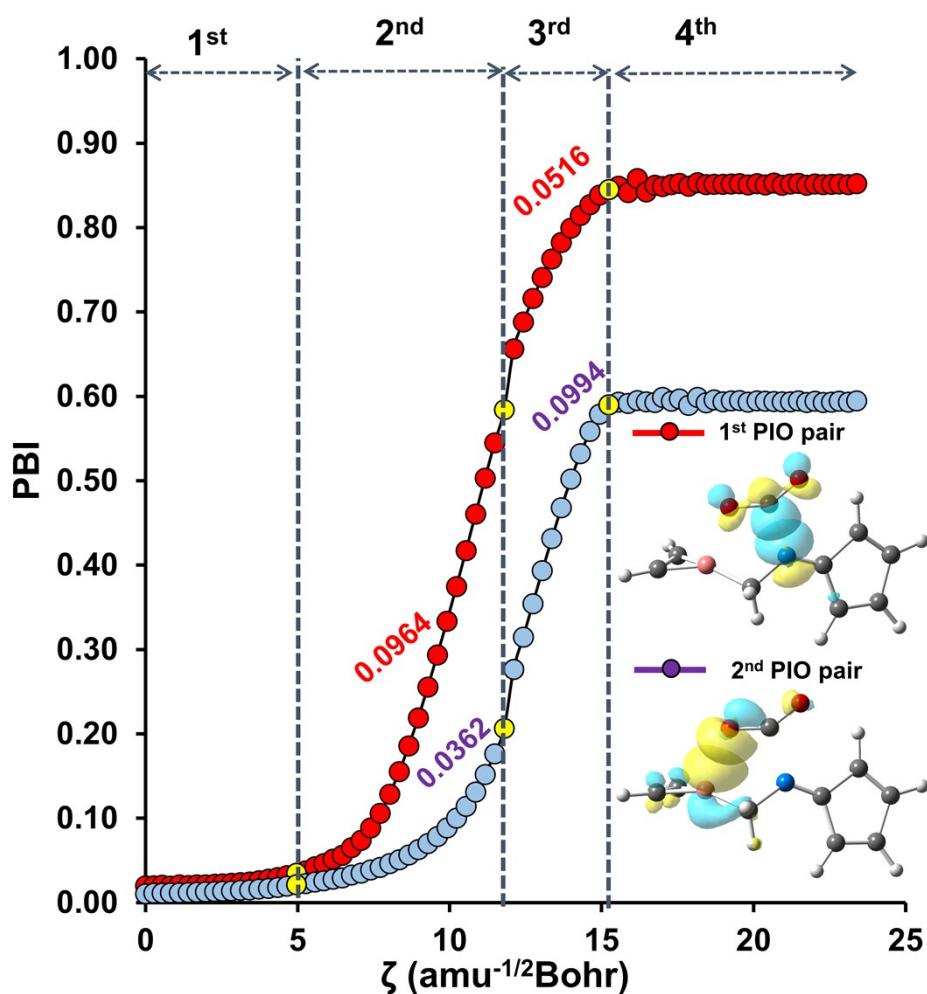


**Figure S12.** PBI vs IRC plots for the reaction of  $\text{CO}_2$  with **5**. (The prominent interacting orbitals are depicted in the respective plots, the slope of the curves in specific regions are given in same colour of the curve, the yellow colour circular markers on the curves represents the point where the change begins in the curve)

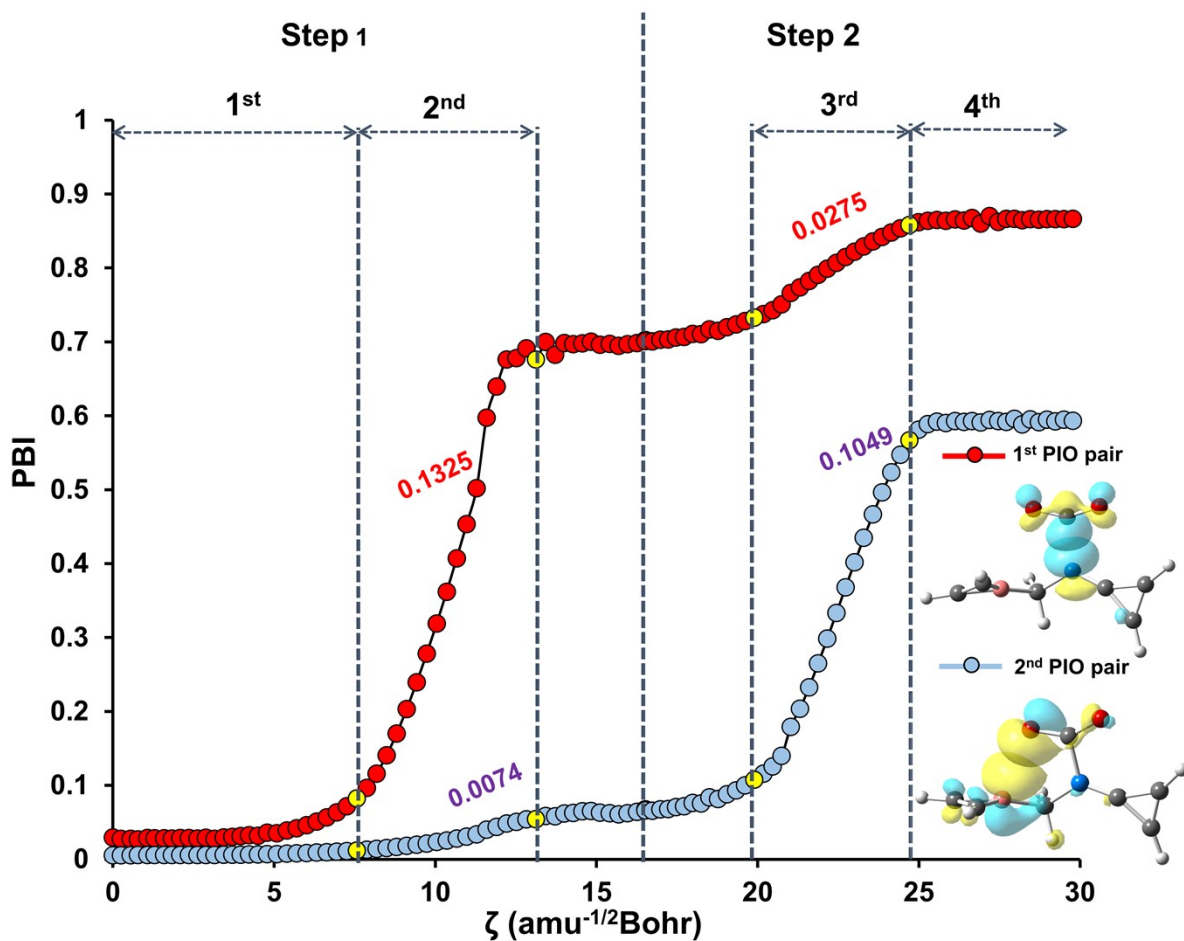


**Figure S13.** PBI vs IRC plots for the reaction of  $\text{CO}_2$  with **6**. (The prominent interacting orbitals are depicted in the respective plots, the slope of the curves in specific regions are given in same colour of the curve, the yellow colour circular markers on the curves represents the point where the change begins in the curve)



## Section S8. Variation in important distances throughout the metadynamics simulation

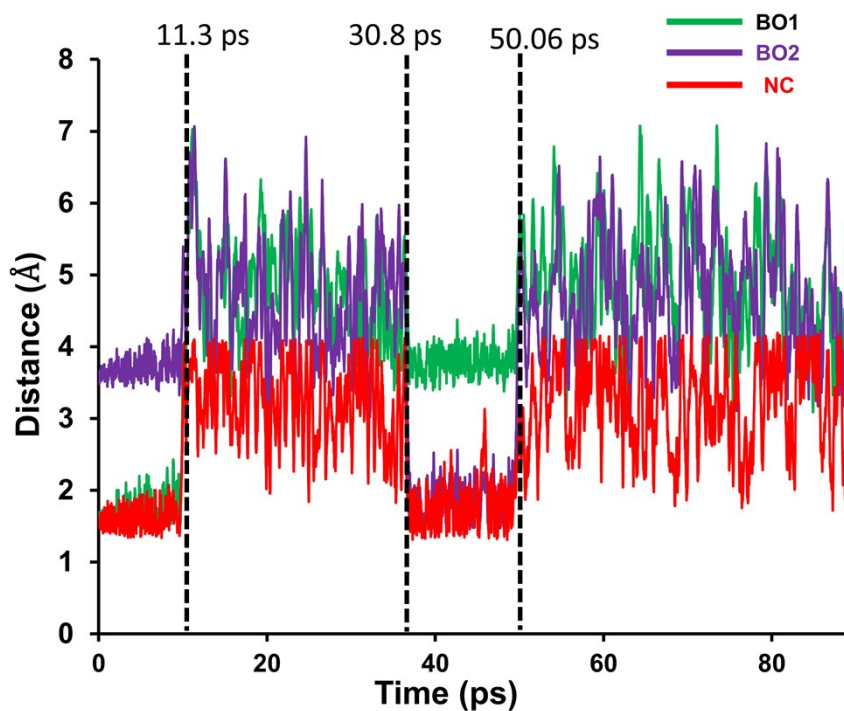


**Figure S14.** Variation of NC, BO1 and BO2 distance with time in the metadynamics simulation of CO<sub>2</sub> with **3**. (O1 and O2 represents the two atoms of the CO<sub>2</sub> molecule)

It can be observed from Figure S12 that CO<sub>2</sub> liberation takes place after 11.3 ps of simulation. The capture of CO<sub>2</sub> occubeen found to be 30.8 ps. Interestingly, the O atom which was not bonded to the B atom in the adduct has found to form the BO bond in the capturing process.



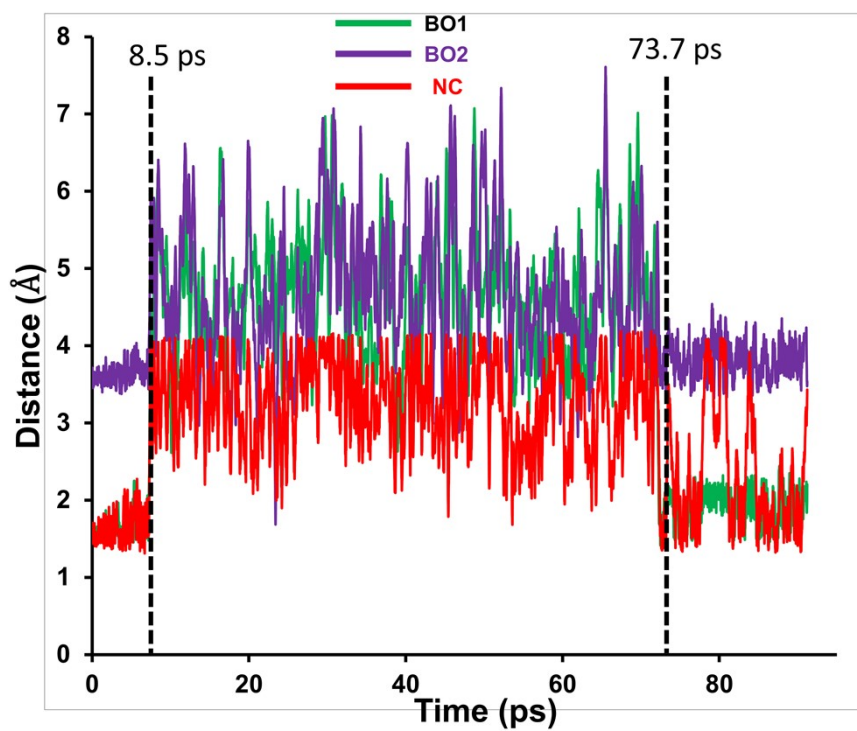


**Figure S15.** Variation of NC, BO1 and BO2 distance with time in the metadynamics simulation of CO<sub>2</sub> with 4. (O1 and O2 represents the two atoms of the CO<sub>2</sub> molecule)

The liberation process appears at 8.5 ps of the simulation and capturing occurs at 73.7 ps.

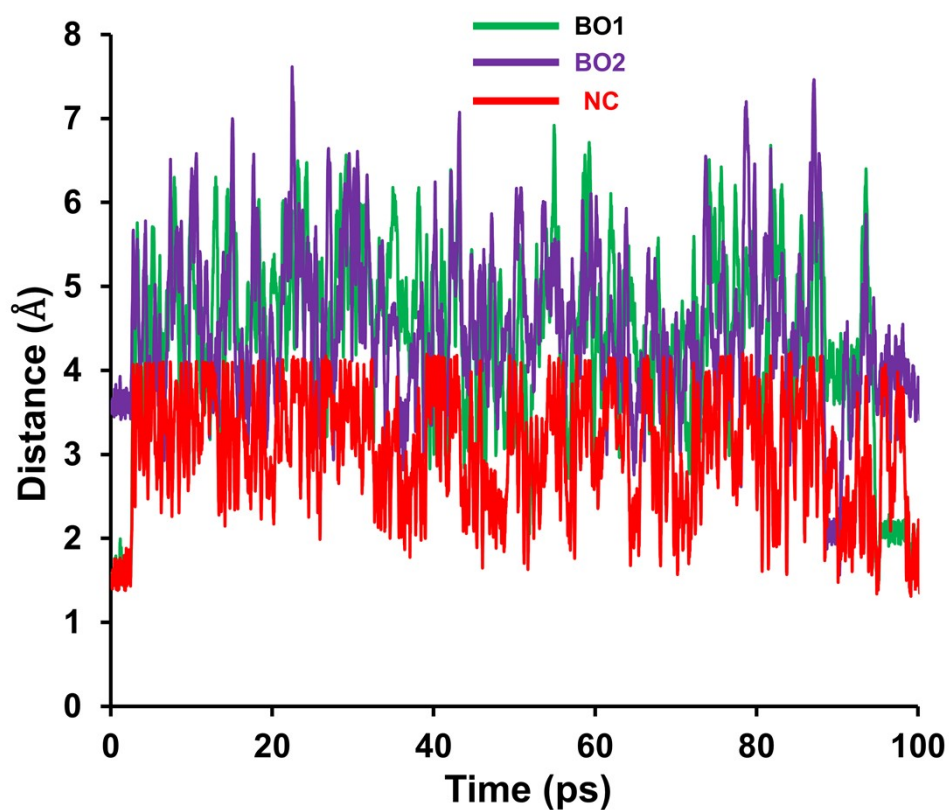


**Figure S16.** Variation of NC, BO1 and BO2 distance with time in the metadynamics simulation of CO<sub>2</sub> with 5. (O1 and O2 represents the two atoms of the CO<sub>2</sub> molecule)

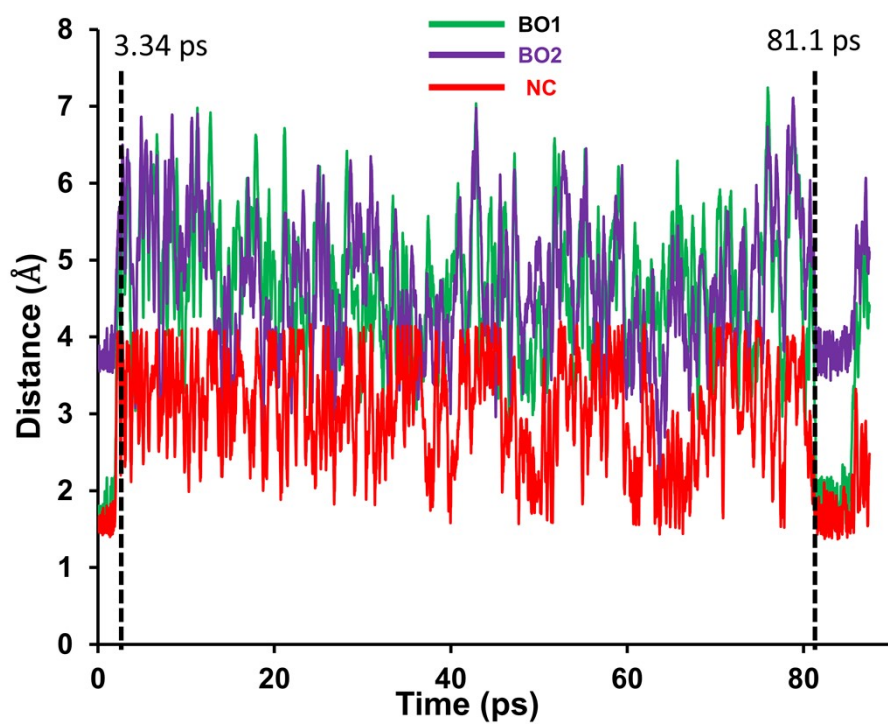


**Figure S17.** Variation of NC, BO1 and BO2 distance with time in the metadynamics simulation of CO<sub>2</sub> with 6. (O1 and O2 represents the two atoms of the CO<sub>2</sub> molecule)

**Section S9. 3-D FES and relative free energy profile along the MEP obtained from the metadynamics simulations**

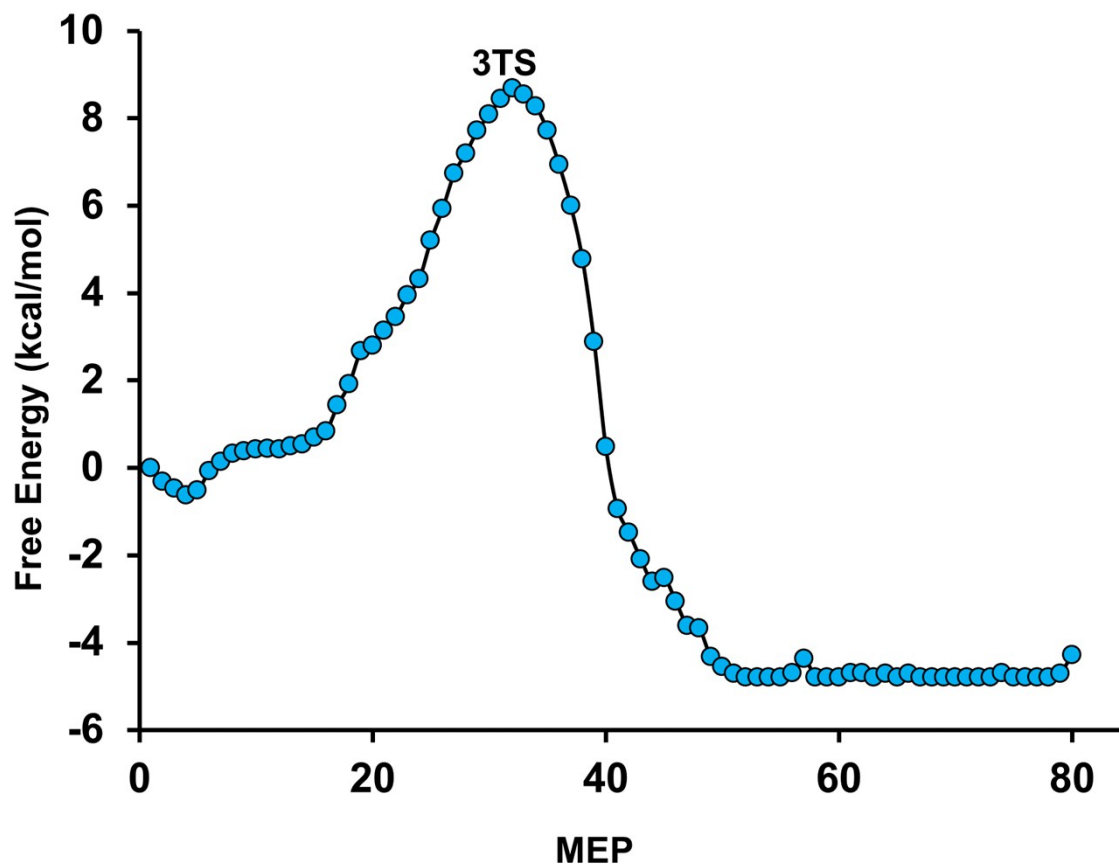


**Figure S18.** Relative free energy profile along the MEP obtained in the metadynamics for the reaction of CO<sub>2</sub> with **3**.

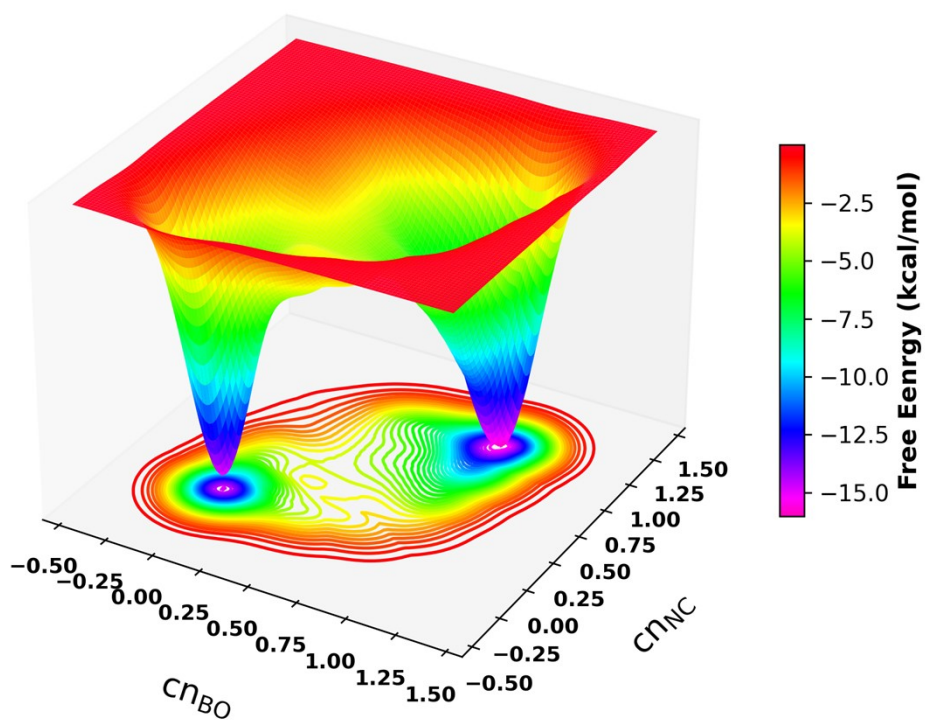


**Figure S19.** 3-Dimensional free energy landscape for the reaction of CO<sub>2</sub> with 4.

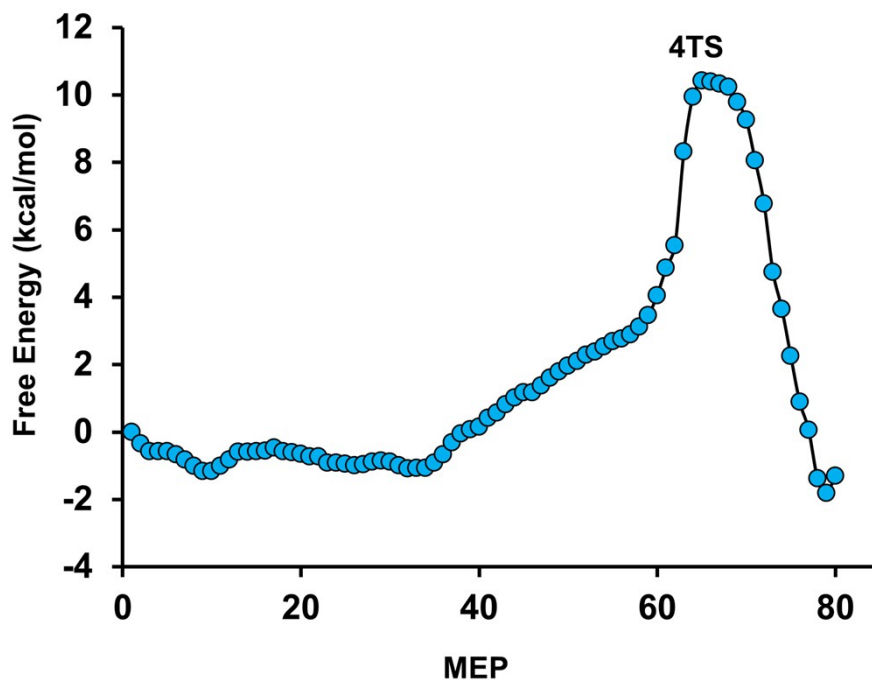


**Figure S20.** Relative free energy profile along the MEP obtained in the metadynamics for the reaction of CO<sub>2</sub> with 4.

## Section S10. FES analysis for the cases of 5 and 6

The valley comprising the adduct 5AD has found to be shallower than the valley consisting 5CM (see Figure S22). This indicates the instability of the CO<sub>2</sub> adduct formed with **5** which has already been indicated by the DFT calculation. This observation also signifies that the unfavourable aromatic modulations at the acidic as well as basic site results in an unstable adduct.

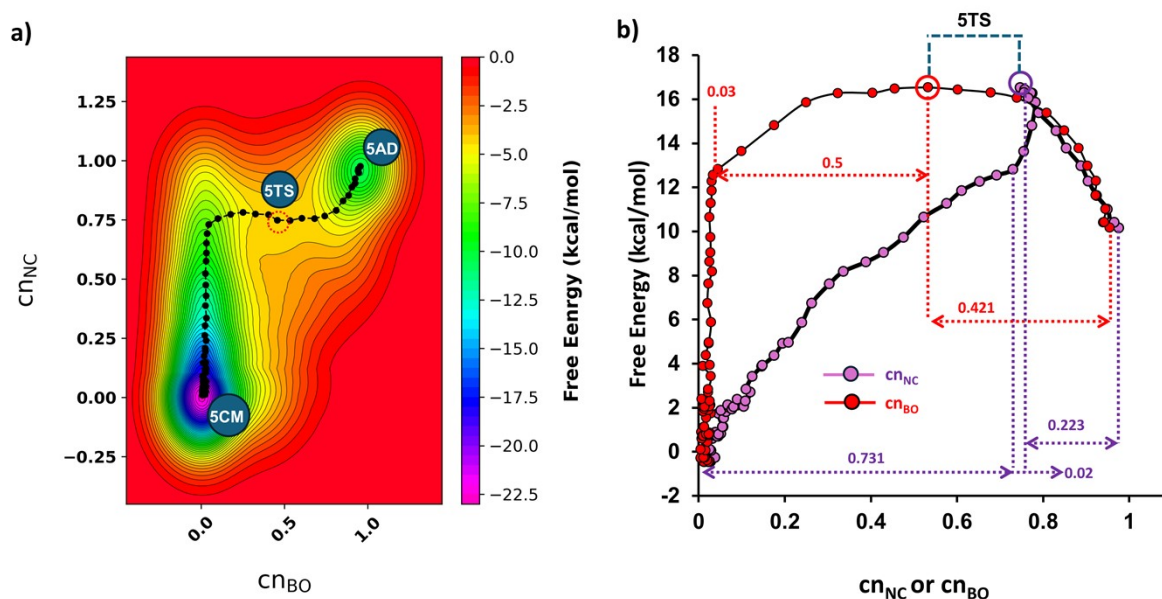


**Figure S21.** a) 2D projection contours of 3D FES for the reaction of CO<sub>2</sub> with **5** and b) variation of free energy with respect to  $cn_{CN}$  and  $cn_{BO}$  along the MEP. (The values of  $\Delta cn_{BO}$  and  $\Delta cn_{NC}$  are depicted in the marked regions of with the respective colours of the curves)

It can be seen from the MEP is 2D contour projection given in Figure S21 a and plot in Figure S21 b that the  $cn_{NC}$  changes from 0 to 0.73 rapidly as the reaction proceeds, while the  $cn_{BO}$  changes ( $\Delta cn_{BO}$ ) only by 0.03 units. However, the increase in the  $cn_{NC}$  has found to be insufficient to bring the transition in the reaction. The transition state 5TS appears when the  $cn_{BO}$  changes by 0.5 units (see Figure S21 b). It is also important to note that the  $cn_{BO}$  value in 5TS has found to be 0.533, while the  $cn_{NC}$  value was 0.746. The higher value of  $cn_{NC}$  than  $cn_{BO}$  justifies the observation of shorter NC distance than BO distance in the 5TS. These results highlight the fact that acidic site controls the kinetics of the reaction of CO<sub>2</sub> with **5**. After the transition stage of the reaction the  $\Delta cn_{BO}$  has found to be 0.421 while  $\Delta cn_{NC}$  has been observed to be 0.223. The higher value of  $\Delta cn_{BO}$  signifies the control of the acidic side after the transition state in the formation of 5AD. The observed free energy profile for the reaction of CO<sub>2</sub> with **5** given in Figure S23 has found to be similar to the IRC path shown in Figure S5. The energy

barrier of 16.52 kcal/mol for the reaction can also be seen from the Figure S20. The energy barrier calculated from the metadynamics is found to be close to the energy barrier relative to the reactant complex calculated from the DFT calculation.

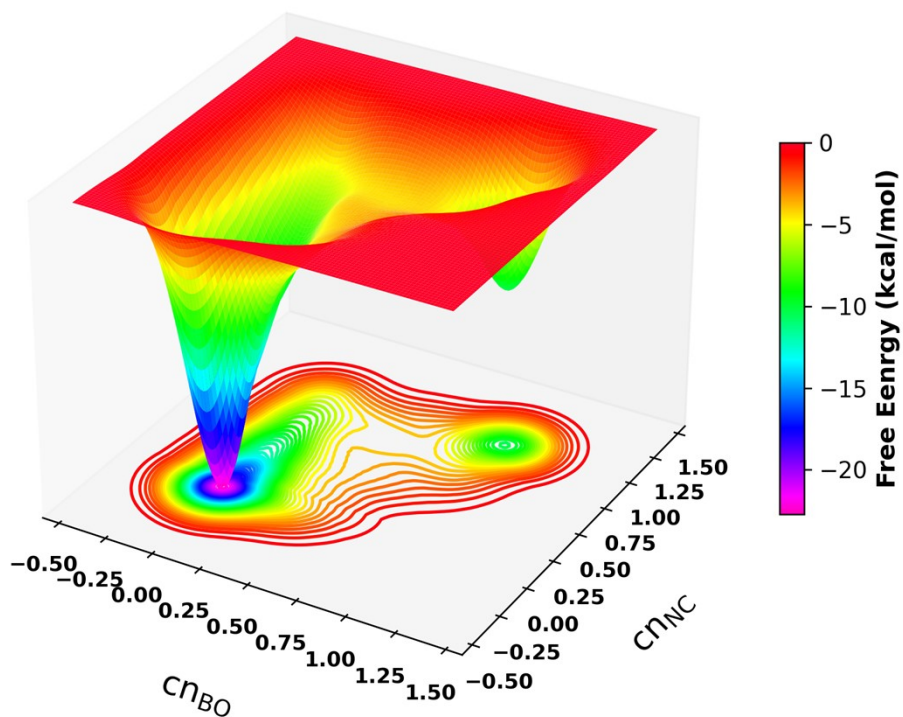


**Figure S22.** 3-Dimensional free energy landscape for the reaction of CO<sub>2</sub> with **5**.

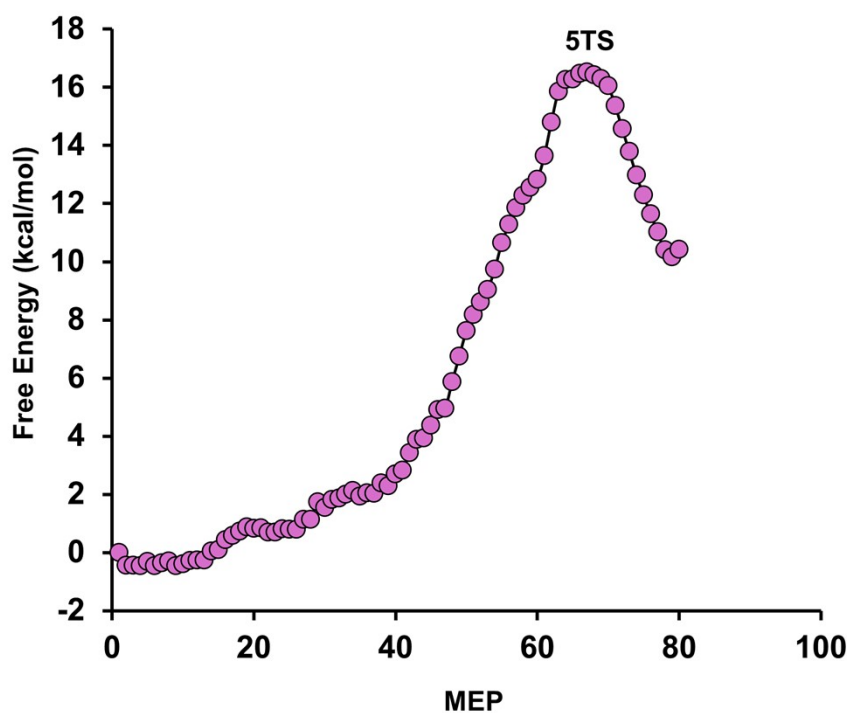




**Figure S23.** Relative free energy profile along the MEP obtained in the metadynamics for the reaction of CO<sub>2</sub> with **5**.

Further in case of **6**, the 3D FES shows shallower valley for the adduct indicating its instability (see Figure S25 in ESI). The MEP on the 2D FES given in Figure S24 indicates the prominence of NC interaction over BO interaction as signified by the rapid increase in  $c_{\text{NC}}$  along the MEP (also see Figure S26 in ESI). However, like **5**, the transition state occurs during the changes in the  $c_{\text{BO}}$  which can also be seen from the Figure S26 in the ESI. This result shows that the reaction kinetics in case of **6** is controlled by the acidic site. The free energy barrier calculated from the energy profile given in Figure S27 is 12.57 kcal/mol which is close to the activation barrier calculated from the DFT based calculations.

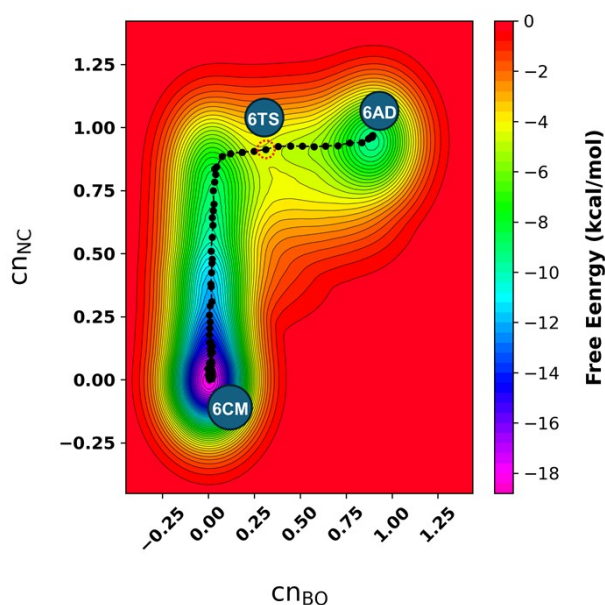


**Figure S24.** 2D projection contours of 3D FES for the reaction of CO<sub>2</sub> with **6**. (Only the transition state (6TS) observed due the change in BO distance has been depicted in the figure).

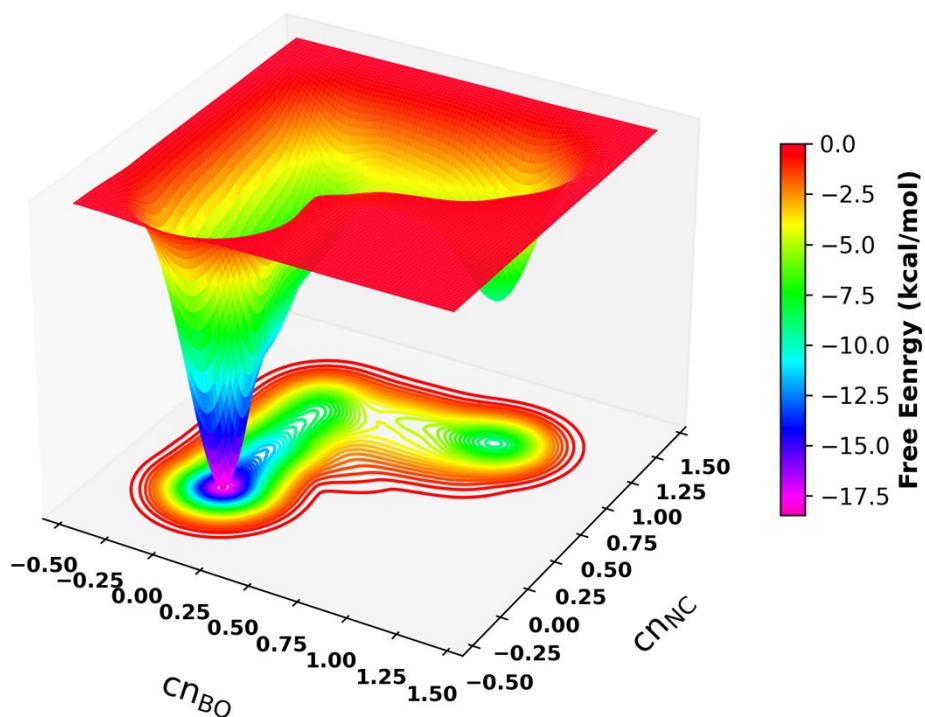


**Figure S25.** 3-Dimensional free energy landscape for the reaction of CO<sub>2</sub> with **6**.

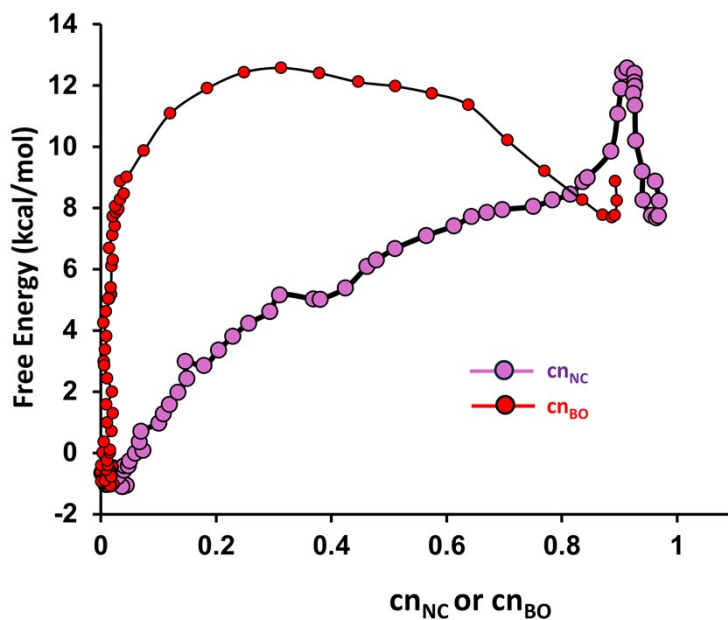


**Figure S26.** Variation of free energy with respect to coordination numbers along the MEP obtained from the metadynamics in case of **6**.



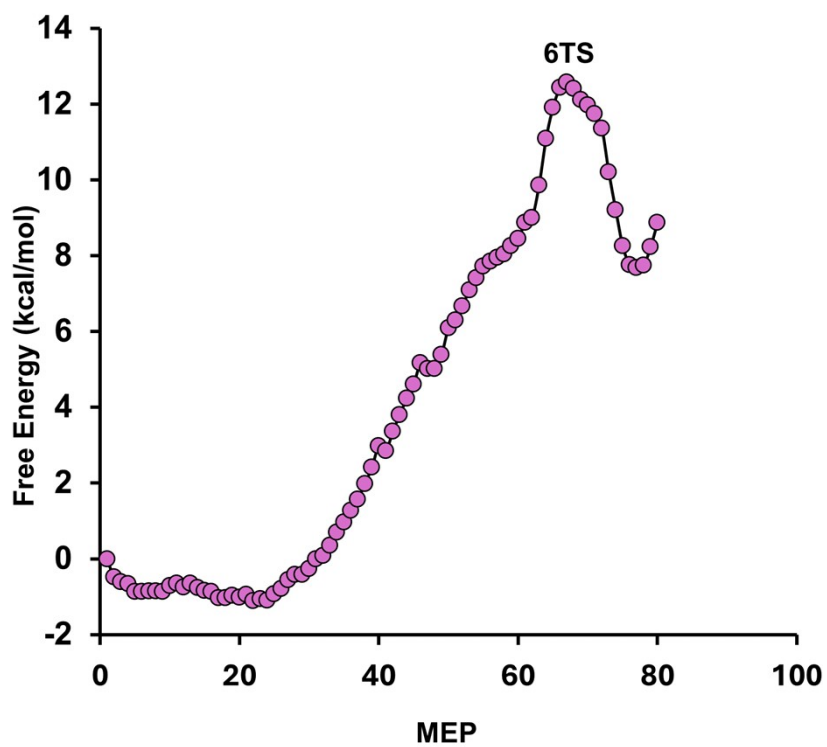


**Figure S27.** Relative free energy profile along the MEP obtained in the metadynamics for the reaction of CO<sub>2</sub> with **6**.

## Section S11. Optimized cartesian coordinates of the structures obtained in the reaction of CO<sub>2</sub> with the proposed IFLPs.

3

C	-2.32706000	-1.16519100	0.14502000
C	-3.28677300	-0.27847900	0.41902500
C	-2.80466900	1.14294100	0.24217700
C	-1.52782700	1.18873100	-0.14596000
H	-2.46883200	-2.23531900	0.21153500
H	-4.30031300	-0.50329100	0.73253800
H	-3.45636000	1.99167100	0.41842900
H	-0.98086700	2.10048700	-0.33688000
B	-1.04500000	-0.31293400	-0.24560700
C	0.35565600	-0.87371600	-0.63437900
H	0.66594400	-1.62967600	0.10663500
H	0.18716200	-1.44924800	-1.55893800
N	1.37824600	0.13120600	-0.88681500
C	2.39515600	0.10777000	-0.15500500
C	3.65501600	0.64063300	0.23097800
C	3.21696200	-0.41071700	0.90559000
H	4.44576500	1.36397300	0.11358300
H	3.42601200	-1.10420600	1.70416600

Zero-point correction=	0.137659
(Hartree/Particle)	
Thermal correction to Energy=	0.147270
Thermal correction to Enthalpy=	0.148214
Thermal correction to Gibbs Free Energy=	0.101161
Sum of electronic and zero-point Energies=	-388.936197
Sum of electronic and thermal Energies=	-388.926586
Sum of electronic and thermal Enthalpies=	-388.925641
Sum of electronic and thermal Free Energies=	-388.972695

3CM

C	-2.49693000	-1.16575900	-0.83126800
C	-3.28136800	-1.00873200	0.23785100
C	-2.51571800	-0.46936900	1.42167500
C	-1.22875800	-0.26578900	1.12891400
H	-2.85355800	-1.53555600	-1.78267400
H	-4.34230700	-1.22547200	0.29468800
H	-2.99597800	-0.28567500	2.37643300
H	-0.50327800	0.11589800	1.83505800
B	-1.04558900	-0.71479800	-0.38059700
C	0.28465200	-0.81853700	-1.19409100
H	0.54066200	-1.89248600	-1.24797200
H	0.10031700	-0.50962000	-2.22853400
N	1.36765900	-0.01131900	-0.64553300
C	2.32474400	-0.60491100	-0.09364700
C	3.56005300	-0.57226500	0.60499900
C	3.05123100	-1.76518100	0.33741500
H	4.36845500	-0.02142500	1.05776300
H	3.17986600	-2.83110800	0.43405900
C	0.01511100	2.33502400	-0.18400900
O	0.71570500	2.72136100	0.64743200
O	-0.73044800	2.01011200	-1.00795000

Zero-point correction=	0.150816
(Hartree/Particle)	
Thermal correction to Energy=	0.164436
Thermal correction to Enthalpy=	0.165380
Thermal correction to Gibbs Free Energy=	0.106530
Sum of electronic and zero-point Energies=	-577.530072
Sum of electronic and thermal Energies=	-577.516452
Sum of electronic and thermal Enthalpies=	-577.515508
Sum of electronic and thermal Free Energies=	-577.574359

### 3TS

C	-2.74497400	-0.27840800	-0.99142100
C	-3.56768700	-0.40452300	0.05365000
C	-2.81434800	-0.54100300	1.35056800
C	-1.49346700	-0.50275400	1.16126600
H	-3.08724100	-0.16566800	-2.01081300
H	-4.65156400	-0.41014200	0.01903900
H	-3.32575800	-0.65003000	2.30037500
H	-0.77207900	-0.57793200	1.96432600
B	-1.28072800	-0.39883100	-0.40877600
C	0.04583200	-0.77450200	-1.17972800
H	0.16577400	-1.86690800	-1.15731800
H	-0.00555000	-0.47438400	-2.22937000
N	1.17219800	-0.09706800	-0.55836300
C	2.18897700	-0.69204500	-0.12375400
C	3.43502600	-0.62952400	0.54046200
C	3.01887800	-1.81943300	0.13338400
H	4.19773100	-0.04984400	1.03290100
H	3.22143600	-2.87589400	0.07157900
C	0.68961400	1.82851300	-0.02844700
O	1.67650800	2.25036800	0.43585600
O	-0.43795900	1.82794500	-0.37762800

Zero-point correction=	0.151451
(Hartree/Particle)	
Thermal correction to Energy=	0.163738
Thermal correction to Enthalpy=	0.164683
Thermal correction to Gibbs Free Energy=	0.111048
Sum of electronic and zero-point Energies=	-577.523302
Sum of electronic and thermal Energies=	-577.511014
Sum of electronic and thermal Enthalpies=	-577.510070
Sum of electronic and thermal Free Energies=	-577.563705

Imaginary Frequencies -- -180.0112

### 3AD

C	-2.49662500	0.03311800	-1.15456800
C	-3.58731100	-0.32442700	-0.46727100
C	-3.29552300	-0.50124800	0.98285700
C	-2.00903200	-0.26458200	1.26230000
H	-2.51461900	0.20498800	-2.22559900
H	-4.58040800	-0.47431900	-0.87801900
H	-4.06367800	-0.78391000	1.69535500
H	-1.61324000	-0.33766300	2.27068100
B	-1.25552700	0.04214800	-0.13400700
C	-0.03668900	-1.02351200	-0.49769700
H	-0.03128200	-1.92636500	0.11007700
H	0.00747700	-1.29214000	-1.55417300

N	1.14614400	-0.20718000	-0.18267300
C	2.35838800	-0.57873600	-0.03579000
C	3.68287200	-0.25876900	0.24599400
C	3.37868900	-1.52928700	-0.00564300
H	4.40512200	0.50134100	0.48935100
H	3.69442900	-2.55342800	-0.11186700
C	0.81564200	1.23816900	-0.02269900
O	1.70471100	2.02475300	0.14267300
O	-0.44366700	1.36982900	-0.10417000

Zero-point correction=	0.155632
(Hartree/Particle)	
Thermal correction to Energy=	0.166688
Thermal correction to Enthalpy=	0.167632
Thermal correction to Gibbs Free Energy=	0.117733
Sum of electronic and zero-point Energies=	-577.555699
Sum of electronic and thermal Energies=	-577.544643
Sum of electronic and thermal Enthalpies=	-577.543699
Sum of electronic and thermal Free Energies=	-577.593598

#### 4

C	-3.07427300	0.59778700	0.51446300
C	-3.61226700	-0.57064800	0.15695300
C	-2.62894600	-1.43336100	-0.60053500
C	-1.44519000	-0.83124600	-0.74307500
H	-3.60949600	1.35954000	1.06409000
H	-4.62380400	-0.90272500	0.36201400
H	-2.89834900	-2.41755200	-0.96691700
H	-0.59900900	-1.27106100	-1.25200100
B	-1.58347700	0.56463400	-0.01974000
C	-0.48546700	1.65215400	0.22881300
H	-0.89244500	2.64306900	0.00843400
H	-0.32923500	1.63805400	1.32093000
N	0.74361200	1.46891500	-0.50670500
C	1.56808900	0.58266600	-0.12947100
C	1.52135700	-0.36811300	1.01444900
C	2.83195300	0.29153100	-0.85031600
H	0.73226200	-0.44036700	1.74594200
C	2.62619500	-1.12193900	0.94807300
H	3.14315000	0.82975900	-1.73129300
C	3.44877300	-0.70938900	-0.21469800
H	2.89609500	-1.91775300	1.62739400
H	4.39158500	-1.16319900	-0.48089900

Zero-point correction=	0.174684
(Hartree/Particle)	
Thermal correction to Energy=	0.185315
Thermal correction to Enthalpy=	0.186259
Thermal correction to Gibbs Free Energy=	0.136848
Sum of electronic and zero-point Energies=	-466.365402
Sum of electronic and thermal Energies=	-466.354771
Sum of electronic and thermal Enthalpies=	-466.353827
Sum of electronic and thermal Free Energies=	sum -466.403238

#### 4CM

C	-1.27801200	-0.62165900	1.05507200
C	-2.44150300	-1.04389900	1.55772600
C	-3.44979500	-1.33746900	0.47273900
C	-2.94802000	-1.11815300	-0.74510200

H	-0.41718200	-0.36450500	1.65848100
H	-2.67755600	-1.17724300	2.60748200
H	-4.45206400	-1.68111900	0.70237200
H	-3.50832700	-1.26152300	-1.65825100
B	-1.45871500	-0.63777500	-0.51647700
C	-0.35253300	-0.38543000	-1.60220600
H	-0.04247700	-1.38382400	-1.95034500
H	-0.79097200	0.12468800	-2.46286000
N	0.73872300	0.40993800	-1.09346700
C	1.72877900	-0.14020800	-0.52314900
C	2.04408500	-1.57383500	-0.28253700
C	2.83416700	0.63304000	0.09573600
H	1.44620400	-2.41502100	-0.59332400
C	3.19292400	-1.61469200	0.40386300
H	2.87477600	1.71050900	0.08484600
C	3.68998700	-0.23700800	0.63974200
H	3.69821100	-2.50629800	0.74641200
H	4.60034500	-0.00431300	1.17141000
C	-0.74764300	2.43856200	0.15177700
O	0.10406200	2.79681500	0.84158600
O	-1.63444500	2.11349100	-0.51802700

Zero-point correction=	0.187821
(Hartree/Particle)	
Thermal correction to Energy=	0.202466
Thermal correction to Enthalpy=	0.203410
Thermal correction to Gibbs Free Energy=	0.142830
Sum of electronic and zero-point Energies=	-654.958428
Sum of electronic and thermal Energies=	-654.943783
Sum of electronic and thermal Enthalpies=	-654.942839
Sum of electronic and thermal Free Energies=	-655.003419

#### 4TS

C	-1.68452900	-0.76229600	1.13403000
C	-2.89837900	-1.29297100	1.31271600
C	-3.79443700	-1.04687100	0.13870000
C	-3.17816300	-0.35594000	-0.82573000
H	-0.88922700	-0.84273400	1.86523100
H	-3.23206500	-1.84669600	2.18331300
H	-4.81687100	-1.40720500	0.11167800
H	-3.65584100	-0.08192300	-1.75738800
B	-1.67688500	-0.16463300	-0.34446000
C	-0.40875300	-0.36903900	-1.30812500
H	-0.21085200	-1.43265600	-1.46362100
H	-0.60745800	0.09665700	-2.27780700
N	0.68350000	0.34299000	-0.69880800
C	1.77375200	-0.18989200	-0.33260100
C	2.26280100	-1.58402000	-0.49351500
C	2.84593200	0.55096300	0.37987600
H	1.72618900	-2.38646300	-0.97108900
C	3.47717900	-1.63874900	0.06397300
H	2.77778000	1.59529400	0.63767000
C	3.84342500	-0.30695900	0.60927200
H	4.11310200	-2.51021100	0.11997000
H	4.77703200	-0.09291800	1.10743300
C	-0.36119100	2.14695300	0.09427700
O	0.47280900	2.87664000	0.41013900
O	-1.42877000	1.67636300	-0.10747400

Zero-point correction=	0.188540
(Hartree/Particle)	
Thermal correction to Energy=	0.201643
Thermal correction to Enthalpy=	0.202587
Thermal correction to Gibbs Free Energy=	0.147299
Sum of electronic and zero-point Energies=	-654.948004
Sum of electronic and thermal Energies=	-654.934902
Sum of electronic and thermal Enthalpies=	-654.933958
Sum of electronic and thermal Free Energies=	-654.989245

Imaginary Frequencies -- -232.9478

#### 4AD

C	-2.01233500	-0.67548200	1.21245600
C	-3.25494200	-1.16844900	1.16126800
C	-3.96884600	-0.74648100	-0.07611700
C	-3.20639100	0.03164700	-0.85334900
H	-1.34455700	-0.87299500	2.04513400
H	-3.72380300	-1.79761800	1.91042900
H	-4.98819500	-1.05257300	-0.28564300
H	-3.55337900	0.43350500	-1.79852900
B	-1.76489200	0.12536100	-0.16584900
C	-0.51592200	-0.48774900	-1.07010800
H	-0.34930500	-1.55785900	-1.01962900
H	-0.62522200	-0.15327500	-2.10509200
N	0.59211800	0.25020700	-0.48804400
C	1.76528800	-0.17923600	-0.20691000
C	2.30358000	-1.49713800	-0.60561800
C	2.81712400	0.51941900	0.57367500
H	1.77570300	-2.22682700	-1.19480100
C	3.54366100	-1.56619900	-0.11780500
H	2.71060400	1.50231100	0.99458500
C	3.86014400	-0.31077800	0.62361000
H	4.22914200	-2.39230900	-0.23368000
H	4.80018500	-0.12199400	1.11943600
C	0.07695800	1.62991200	-0.04887500
O	0.84870900	2.51681500	0.13488600
O	-1.18639100	1.55375800	0.02261100

Zero-point correction=	0.191755
(Hartree/Particle)	
Thermal correction to Energy=	0.203965
Thermal correction to Enthalpy=	0.204909
Thermal correction to Gibbs Free Energy=	0.152518
Sum of electronic and zero-point Energies=	-654.967582
Sum of electronic and thermal Energies=	-654.955372
Sum of electronic and thermal Enthalpies=	-654.954428
Sum of electronic and thermal Free Energies=	-655.006819

#### 5

C	-1.22910400	-0.75714400	-0.98182700
H	-1.68739400	-1.63364200	-1.44836500
H	-0.95955900	-0.07598700	-1.79756500
N	-0.09315700	-1.20379000	-0.20425100
C	0.93780600	-0.47196600	-0.11314900

C	1.25083900	0.86238400	-0.69443300
C	2.12719500	-0.85526300	0.68732200
H	0.60290900	1.44688600	-1.32694900
C	2.47394700	1.20256700	-0.26903000
H	2.19405600	-1.78467300	1.22985200
C	3.02601600	0.12898800	0.59140000
H	2.99773900	2.11805600	-0.50414700
H	4.00144800	0.16374000	1.05297000
C	-2.86223600	0.43850500	1.16448100
C	-3.62237000	0.59665200	0.06633500
H	-2.90588600	0.66371000	2.21912600
H	-4.58231800	1.01468500	-0.19756900
B	-2.32429000	-0.07091600	-0.10083800

Zero-point correction= 0.140155  
(Hartree/Particle)  
Thermal correction to Energy= 0.149357  
Thermal correction to Enthalpy= 0.150301  
Thermal correction to Gibbs Free Energy= 0.103707  
Sum of electronic and zero-point Energies= -388.987640  
Sum of electronic and thermal Energies= -388.978438  
Sum of electronic and thermal Enthalpies= -388.977494  
Sum of electronic and thermal Free Energies= -389.024088

#### 5CM

C	0.72099200	-0.97367000	-1.10441300
H	1.29382400	-0.58328400	-1.95150100
H	0.15999800	-1.84014000	-1.47003900
N	-0.11407900	0.09649400	-0.60672100
C	-1.31982600	-0.11414700	-0.27672900
C	-2.14831700	-1.35024700	-0.31494700
C	-2.19708100	0.95079900	0.27131500
H	-1.82647500	-2.32088000	-0.65417300
C	-3.35771500	-1.02799200	0.15953000
H	-1.86332700	1.96546700	0.41909400
C	-3.39185800	0.40920500	0.52438500
H	-4.19714000	-1.69953500	0.26931100
H	-4.25806100	0.91068200	0.92919000
C	2.88127000	-2.28546000	0.40483800
C	2.40980100	-1.38073300	1.28044700
H	3.64586300	-3.04643900	0.36254300
H	2.60700100	-1.05325300	2.28991000
B	1.77146000	-1.43279900	-0.03922300
C	1.56353300	2.19856700	-0.06911500
O	0.77234700	2.82251100	0.49465900
O	2.40450000	1.62723700	-0.62003800

Zero-point correction= 0.153041  
(Hartree/Particle)  
Thermal correction to Energy= 0.166394  
Thermal correction to Enthalpy= 0.167338  
Thermal correction to Gibbs Free Energy= 0.108877  
Sum of electronic and zero-point Energies= -577.580231  
Sum of electronic and thermal Energies= -577.566879  
Sum of electronic and thermal Enthalpies= -577.565934  
Sum of electronic and thermal Free Energies= -577.624396

#### 5TS

C	0.92476000	-0.85944500	-0.92875300
---	------------	-------------	-------------

H	1.14149100	-0.58690900	-1.96497100
H	0.55054600	-1.88157500	-0.90369600
N	-0.05981900	0.08228100	-0.43778100
C	-1.26866600	-0.19021900	-0.15796100
C	-1.96770200	-1.48996500	-0.33885000
C	-2.26200300	0.75359700	0.42575900
H	-1.53052900	-2.38288200	-0.75119900
C	-3.22130100	-1.31906500	0.08533000
H	-2.04634000	1.77829200	0.66787300
C	-3.40284900	0.07711600	0.56666800
H	-4.00024300	-2.06720200	0.08552200
H	-4.32843900	0.46309900	0.96621600
C	3.66369800	-1.07626000	0.10397700
C	2.92546000	-1.05302100	1.21625100
H	4.68289100	-1.27489100	-0.19057300
H	3.05038200	-1.21908100	2.27559600
B	2.23882600	-0.71312700	-0.05233800
C	0.74125300	1.65101300	-0.15809900
O	-0.05073300	2.52844200	-0.07580200
O	1.91435200	1.37134600	-0.14226500

Zero-point correction=	0.154148
(Hartree/Particle)	
Thermal correction to Energy=	0.165539
Thermal correction to Enthalpy=	0.166483
Thermal correction to Gibbs Free Energy=	0.115849
Sum of electronic and zero-point Energies=	-577.557157
Sum of electronic and thermal Energies=	-577.545767
Sum of electronic and thermal Enthalpies=	-577.544823
Sum of electronic and thermal Free Energies=	-577.595456

Imaginary Frequencies -- -283.6147

## 5AD

C	0.93579200	-0.97538100	-0.72902700
H	1.06265300	-0.94063300	-1.81557900
H	0.62155200	-1.96591900	-0.41748600
N	-0.06725800	0.02091600	-0.38186100
C	-1.30548100	-0.17210100	-0.12270000
C	-2.01539700	-1.45820200	-0.29576900
C	-2.28440900	0.81298500	0.40414000
H	-1.57131500	-2.36066800	-0.67873400
C	-3.27932000	-1.25087000	0.07813800
H	-2.05269800	1.83754300	0.62975400
C	-3.44369800	0.16378900	0.52236800
H	-4.07565200	-1.97996900	0.06556300
H	-4.37185100	0.58009000	0.88347900
C	3.72811200	-0.81381500	-0.04835900
C	3.13649800	-0.93529500	1.12776400
H	4.70010800	-0.98923100	-0.48732200
H	3.38751500	-1.25786400	2.12867100
B	2.27450400	-0.37119800	-0.00194700
C	0.63358800	1.38183900	-0.19137600
O	-0.01922600	2.37915700	-0.22477900
O	1.86470900	1.15440900	-0.03730200

Zero-point correction=	0.155995
(Hartree/Particle)	
Thermal correction to Energy=	0.166849
Thermal correction to Enthalpy=	0.167794



Thermal correction to Gibbs Free Energy=	0.118852
Sum of electronic and zero-point Energies=	-577.566365
Sum of electronic and thermal Energies=	-577.555511
Sum of electronic and thermal Enthalpies=	-577.554567
Sum of electronic and thermal Free Energies=	-577.603508

## 6

C	0.42847700	1.02068400	-0.17428800
H	0.10281700	1.37309900	0.81633000
H	0.68713200	1.92466900	-0.73652200
N	-0.63032200	0.31646300	-0.89170700
C	-1.64935400	0.00384300	-0.23398200
C	-2.93273000	-0.60278400	-0.15254200
C	-2.45798700	-0.05533900	0.95511300
H	-3.75069600	-1.13703000	-0.60842800
H	-2.64500600	0.14436800	1.99796700
C	2.55954300	-1.02037400	-0.14643500
C	3.12493200	0.03342900	0.46706400
H	2.82433000	-2.02736200	-0.43184100
H	4.07218900	0.28836700	0.91930000
B	1.73683900	0.18837800	-0.00088700

Zero-point correction=	0.103157
(Hartree/Particle)	
Thermal correction to Energy=	0.111271
Thermal correction to Enthalpy=	0.112215
Thermal correction to Gibbs Free Energy=	0.069125
Sum of electronic and zero-point Energies=	-311.558563
Sum of electronic and thermal Energies=	-311.550449
Sum of electronic and thermal Enthalpies=	-311.549505
Sum of electronic and thermal Free Energies=	-311.592595

## 6CM

C	0.78483400	-1.08961800	0.96084600
H	0.65347600	-2.18045300	0.91381100
H	1.01969000	-0.86430700	2.00686400
N	-0.42910000	-0.36778700	0.59307700
C	-1.38302600	-1.02644100	0.11316200
C	-2.69070100	-1.06942300	-0.43388500
C	-2.04565400	-2.22094100	-0.32578900
H	-3.59020000	-0.56178500	-0.74135700
H	-2.08410300	-3.28513900	-0.49351600
C	3.45384100	-0.77742500	-0.24233900
C	2.69505600	0.06361100	-0.96604300
H	4.48573300	-1.09277900	-0.19508700
H	2.81274400	0.75833400	-1.78394600
B	2.02676600	-0.68653500	0.10555000
C	-0.69079800	2.23627900	0.05362600
O	-1.74834800	2.04503100	-0.37586000
O	0.35224800	2.52210200	0.45791900

Zero-point correction=	0.116074
(Hartree/Particle)	
Thermal correction to Energy=	0.128337
Thermal correction to Enthalpy=	0.129281
Thermal correction to Gibbs Free Energy=	0.073707
Sum of electronic and zero-point Energies=	-500.152086
Sum of electronic and thermal Energies=	-500.139823
Sum of electronic and thermal Enthalpies=	-500.138879

Sum of electronic and thermal Free Energies= -500.194453

**6TS1**

C	-0.63931600	-0.83515400	-0.98050600
H	-0.41735700	-1.90078800	-1.10239300
H	-0.82002600	-0.42884800	-1.97806700
N	0.50434100	-0.13847700	-0.40956200
C	1.57262500	-0.70896400	-0.06229400
C	2.85564800	-0.59727300	0.49915100
C	2.45411500	-1.80210500	0.12002800
H	3.61332300	0.03452800	0.92966500
H	2.67613000	-2.85253400	0.03211800
C	-3.38064500	-0.77953000	0.09099300
C	-2.63469600	-0.42075200	1.14919400
H	-4.42145800	-0.93762700	-0.14773600
H	-2.77502500	-0.14445700	2.18292600
B	-1.93167200	-0.66908900	-0.11395800
C	0.33791900	1.65063100	-0.10165500
O	1.36927700	2.00910700	0.37366900
O	-0.75946600	1.92881600	-0.46982600

Zero-point correction= 0.117005  
(Hartree/Particle)  
Thermal correction to Energy= 0.127732  
Thermal correction to Enthalpy= 0.128676  
Thermal correction to Gibbs Free Energy= 0.079024  
Sum of electronic and zero-point Energies= -500.143942  
Sum of electronic and thermal Energies= -500.133215  
Sum of electronic and thermal Enthalpies= -500.132271  
Sum of electronic and thermal Free Energies= -500.181923

Imaginary Frequencies -- -140.2459

**6TS2**

C	-0.54826600	-1.02518100	-0.77885600
H	-0.32834500	-2.06814800	-0.53983700
H	-0.60833300	-0.92926500	-1.86459400
N	0.54306200	-0.17661300	-0.30751600
C	1.71072000	-0.57648200	-0.01591900
C	2.99173900	-0.25753300	0.43775000
C	2.73310400	-1.52629600	0.14447400
H	3.66873400	0.50805000	0.77455500
H	3.07609300	-2.54509100	0.07826700
C	-2.74894900	-0.49593900	1.10698500
C	-3.37053900	-0.57599300	-0.07549600
H	-3.00499000	-0.40128500	2.15134800
H	-4.37782400	-0.58271700	-0.46314500
B	-1.89796500	-0.58106600	-0.09528900
C	0.19786200	1.38672800	-0.13912100
O	-0.98650300	1.54200000	-0.37299400
O	1.17013100	2.03103200	0.17468800

Zero-point correction= 0.118389  
(Hartree/Particle)  
Thermal correction to Energy= 0.128333  
Thermal correction to Enthalpy= 0.129278  
Thermal correction to Gibbs Free Energy= 0.082529  
Sum of electronic and zero-point Energies= -500.142443

Sum of electronic and thermal Energies=	-500.132499
Sum of electronic and thermal Enthalpies=	-500.131554
Sum of electronic and thermal Free Energies=	-500.178303

Imaginary Frequencies -- -115.7448

**6AD1**

C	-0.61150300	-0.88080600	-0.93163500
H	-0.37176300	-1.94791900	-0.94469500
H	-0.75277500	-0.56022700	-1.96504200
N	0.51171700	-0.13344900	-0.37597700
C	1.61966400	-0.64706300	-0.04427900
C	2.89806900	-0.46097200	0.49119300
C	2.55306400	-1.68848900	0.12448700
H	3.61792700	0.22540200	0.90183700
H	2.81807900	-2.72835700	0.03179100
C	-3.38264800	-0.69303100	0.04569700
C	-2.65579100	-0.45968900	1.14985800
H	-4.42095800	-0.77322200	-0.23779000
H	-2.81615200	-0.25537300	2.19728800
B	-1.92439300	-0.64494700	-0.10902200
C	0.28969800	1.50457900	-0.12361800
O	1.30134800	1.99056400	0.31414000
O	-0.83856500	1.77836100	-0.44872300

Zero-point correction=	0.118083
(Hartree/Particle)	
Thermal correction to Energy=	0.129102
Thermal correction to Enthalpy=	0.130046
Thermal correction to Gibbs Free Energy=	0.080164
Sum of electronic and zero-point Energies=	-500.143110
Sum of electronic and thermal Energies=	-500.132091
Sum of electronic and thermal Enthalpies=	-500.131146
Sum of electronic and thermal Free Energies=	-500.181029

**6AD2**

C	-0.49902400	-1.22458400	-0.00028800
H	-0.41795200	-1.85166300	0.88818800
H	-0.41810200	-1.85131500	-0.88903400
N	0.60617700	-0.25385500	-0.00021400
C	1.86154100	-0.48218600	0.00014200
C	3.16675000	-0.00041200	0.00020700
C	2.97952300	-1.31755700	0.00003700
H	3.82171600	0.85373200	0.00033600
H	3.39418100	-2.31148100	-0.00002000
C	-3.18786000	-0.44079000	0.66101000
C	-3.18807800	-0.44078500	-0.66058800
H	-3.90352800	-0.53248700	1.46702600
H	-3.90392600	-0.53244600	-1.46644500
B	-1.82190300	-0.25091700	-0.00002300
C	0.13670600	1.16647900	-0.00009700
O	-1.12589900	1.17126900	-0.00011200
O	0.96046700	2.04076100	-0.00001100

Zero-point correction=	0.119888
(Hartree/Particle)	
Thermal correction to Energy=	0.129584
Thermal correction to Enthalpy=	0.130529
Thermal correction to Gibbs Free Energy=	0.083915

Sum of electronic and zero-point Energies=	-500.154884
Sum of electronic and thermal Energies=	-500.145188
Sum of electronic and thermal Enthalpies=	-500.144244
Sum of electronic and thermal Free Energies=	-500.190857